

# **Massachusetts Institute of Technology Reactor LEU Fuel Element Flow Test Conceptual Design**

---

**Nuclear Science & Engineering Division**

## **About Argonne National Laboratory**

Argonne is a U.S. Department of Energy laboratory managed by UChicago Argonne, LLC under contract DE-AC02-06CH11357. The Laboratory's main facility is outside Chicago, at 9700 South Cass Avenue, Lemont, Illinois 60439. For information about Argonne and its pioneering science and technology programs, see [www.anl.gov](http://www.anl.gov).

## **DOCUMENT AVAILABILITY**

**Online Access:** U.S. Department of Energy (DOE) reports produced after 1991 and a growing number of pre-1991 documents are available free at OSTI.GOV (<http://www.osti.gov/>), a service of the U.S. Dept. of Energy's Office of Scientific and Technical Information.

### **Reports not in digital format may be purchased by the public from the National Technical Information Service (NTIS):**

U.S. Department of Commerce  
National Technical Information Service  
5301 Shawnee Rd  
Alexandria, VA 22312  
**[www.ntis.gov](http://www.ntis.gov)**  
Phone: (800) 553-NTIS (6847) or (703)  
605-6000 Fax: (703) 605-6900  
Email: **[orders@ntis.gov](mailto:orders@ntis.gov)**

### **Reports not in digital format are available to DOE and DOE contractors from the Office of Scientific and Technical Information (OSTI):**

U.S. Department of Energy  
Office of Scientific and Technical Information  
P.O. Box 62  
Oak Ridge, TN 37831-0062  
**[www.osti.gov](http://www.osti.gov)**  
Phone: (865) 576-8401  
Fax: (865) 576-5728  
Email: **[reports@osti.gov](mailto:reports@osti.gov)**  
**Disclaimer**

## **Disclaimer**

This report was prepared as an account of work sponsored by an agency of the United States Government. Neither the United States Government nor any agency thereof, nor UChicago Argonne, LLC, nor any of their employees or officers, makes any warranty, express or implied, or assumes any legal liability or responsibility for the accuracy, completeness, or usefulness of any information, apparatus, product, or process disclosed, or represents that its use would not infringe privately owned rights. Reference herein to any specific commercial product, process, or service by trade name, trademark, manufacturer, or otherwise, does not necessarily constitute or imply its endorsement, recommendation, or favoring by the United States Government or any agency thereof. The views and opinions of document authors expressed herein do not necessarily state or reflect those of the United States Government or any agency thereof, Argonne National Laboratory, or UChicago Argonne, LLC.

# Massachusetts Institute of Technology Reactor LEU Fuel Element Flow Test Conceptual Design

---

prepared by

Cezary Bojanowski<sup>1</sup>, Guanyi Wang<sup>1</sup>, Ron Kmak<sup>1</sup>, Andrew Hebden<sup>1</sup>, Aaron Weiss<sup>2</sup>,  
Wade Marcum<sup>2</sup>, David Jaluvka<sup>1</sup>, Lin-wen Hu<sup>3</sup>, Erik Wilson<sup>1</sup>

<sup>1</sup>Nuclear Science & Engineering Division, Argonne National Laboratory

<sup>2</sup>School of Nuclear Science & Engineering, Oregon State University

<sup>3</sup>Nuclear Reactor Laboratory, Massachusetts Institute of Technology

September 2021

(This page left intentionally blank)

## Executive Summary

As part of the U.S. National Nuclear Security Administration's (NNSA's) mission to minimize the civilian use of weapon-grade highly enriched uranium (HEU) fuels, the NNSA Office of Material Management and Minimization (M<sup>3</sup>) Conversion Program is collaborating with six U.S. High Performance Research Reactors (USHPRR), including one critical facility, to convert from the use of HEU to low-enriched uranium (LEU) fuel. The M<sup>3</sup> conversion objectives for the USHPRR are to develop LEU fuel element designs that will ensure safe reactor operations and maintain the existing experimental performance of each facility. The work is being conducted through many interrelated activities that are being completed by stakeholders across organizations.

Within the Reactor Conversion (RC) Pillar of the USHPRR Project, four of the USHPRR, including the Massachusetts Institute of Technology Reactor (MITR-II, also referred to as MITR), have progressed through preliminary element design using the proposed monolithic alloy of uranium-10 wt% molybdenum (U-10Mo). Preliminary fuel element design and safety analyses have been completed for MITR. This work has relied on preliminary data for properties, performance, and fabrication tolerances for the fuel systems that have been produced by the Fuel Qualification (FQ) and Fuel Fabrication (FF) Pillars.

The HEU fuel elements have been operating within the MITR for several decades with excellent performance history. MITR LEU fuel elements have been designed to include 19 fuel plates (four more than the HEU element). The MITR LEU fuel plates have no fins on their surface, and their thickness is reduced from 60 mil (80 mil with fins) for HEU plates to 49 mil. The LEU element design is designated FYT since three different fuel-core thicknesses (F-full, Y-intermediate, T-thin) were designed to address power peaking. Each plate has the same overall plate thickness. Due to the change in the fuel system, to maintain equivalent performance for the reactor facility, the power of the proposed LEU core was increased from that of the HEU core by 1 MW to 7 MW. To maintain safe temperatures in the fuel core and the cladding surface of the unfinned LEU plates, the primary coolant flow rate for the LEU reactor cores has been increased by 20% as compared to the HEU core, from 2000 gpm to 2400 gpm. The changes in the plates' geometry, together with the increased flow rate, create less favorable conditions for the MITR LEU fuel plates from the perspective of hydro-mechanical stability as compared to the conditions for the MITR HEU fuel plates.

In preparation for licensing, a hydraulic performance evaluation of the MITR LEU fuel element will be performed by the RC pillar. The purpose of that hydraulic performance evaluation of the MITR LEU fuel element is to test a prototypic commercially fabricated LEU fuel element, to determine whether any failure modes are observed in the fuel element, including significant deformations such as plate bending, twisting, or plate detachment from the side plate under selected safety basis limits for reactor flow conditions. The evaluation will be performed by a combination of out-of-pile flow test and supporting analyses.

This report describes the activities completed during the conceptual design of the MITR LEU fuel element flow test. Three goals have been identified for the conceptual flow test design:

1. Review the hydraulic reactor design parameters and identify the most limiting conditions for the fuel elements,
2. Review and select the methods and sensors used for monitoring various hydraulic and mechanical characteristics of the flow test, and
3. Develop a conceptual design of the basket to be used in the flow test.

The design parameters for hydraulic testing of the LEU fuel element were reviewed and documented in a separate report. These relate to the design needs of the reactor and, are therefore, referred to as reactor design parameters since they do not take into account design margins required for the experimental test design and other purposes. Here, only a summary of that review containing the information affecting the design of the flow test is included. The most limiting flow conditions in the MITR LEU core is expected to occur with the least number of fuel elements in the core, which is 22 elements. The most limiting plates, from the perspective of flow-induced deflections, in the MITR LEU fuel element are the outermost plates #1 or #19. The most limiting pressure differential acting on these plates occurs when two end channels from adjacent fuel elements are facing each other, creating the largest channel thickness disparity for the outermost plates. The normal operating conditions of the proposed MITR LEU core, including the coolant temperature, system pressure, and coolant chemistry specification, are also summarized (see Section 3 for details).

The expected behavior of the limiting plates in the MITR LEU fuel element has been described based on the prior experimental work and recently performed preliminary fluid-structure interaction analysis for the MITR LEU fuel plates. The flow test of the MITR LEU fuel element will be executed at conservative flow rates for the MITR core (from the hydro-mechanical performance perspective). For these flow rates, the coolant channel flow velocities are a fraction of Miller's critical velocity. Hence, pressure-induced quasi-static deflection is the expected type of response of the MITR LEU fuel plates to the hydrodynamic load of the flowing coolant (oscillations of negligible magnitude are expected). The maximum deflections that are expected to occur at the leading edge of the plate are predicted to be in the order of 50 micrometer (~2 mil). This behavior has a direct impact on the selection of the sensors for monitoring the plate's deflections during the flow test (see Section 3.3 for details).

In light of the historical experiments, prior experimental work under USHPRR Project, and the needs of the currently designed flow test, sensors for monitoring the fuel element, and in particular plate deflections, have been reviewed. Most of the past experiments made use of strain gauges installed on the surface, or embedded in the plates, to measure the deflections indirectly from strains. This technique was proven to work for the detection of static deflections as well as dynamic flutter. However, the past experiments were mostly focused on characterizing the response of the plates to significant coolant flow rates that reach or even exceed Miller's critical velocity. Sensors that are potentially able to resolve the small deflections expected during the flow test of the MITR LEU fuel element have been identified and will be tested under dry and wet conditions to demonstrate their capabilities before the flow test of the MITR LEU fuel element. The demonstration tests are planned for the preliminary flow test design (see Sections 2 and 4 for details).

A conceptual design of the testing vehicle (basket) has been completed and is also described in this report. The flow test will be performed at the Hydro-Mechanical Fuel Test Facility (HMFTF) at Oregon State University (OSU). The external dimensions of the basket allow for its insertion into the HMFTF flow loop. The internal dimensions of the basket represent the most limiting configuration in the core. The final selection of the sensors used for visualization and deflection measurement will be performed during the preliminary design of the flow test. The access to the most limiting plate through the basket walls will be adjusted based on that selection. The design of the basket considers different stages of the planned tests and envisions constraining the element for a portion of the test to prevent lateral and axial motion of the tested fuel element so the displacements of the plates due to the hydrodynamic load can be decoupled from the motion of the fuel element within the basket. The basket design also allows for inspection of the channel gaps thicknesses with a channel gap probe between different stages of the test (see Section 5 for details).

Lastly, activities conducted in preparation for the preliminary flow test design have also been briefly discussed in this report (see Sections 4.5 and 6 for details).

# Table of Contents

<b>Executive Summary .....</b>	<b>i</b>
<b>Table of Contents .....</b>	<b>iii</b>
<b>List of Figures .....</b>	<b>v</b>
<b>List of Tables .....</b>	<b>vii</b>
<b>1 Overview .....</b>	<b>1</b>
1.1 Massachusetts Institute of Technology Reactor and Fuel Element.....	1
1.2 Functions and Requirements for the LEU Fuel Elements.....	4
1.3 Flow Test Goal .....	5
1.4 Flow Test Conceptual Design Goal .....	5
<b>2 Experimental Methods.....</b>	<b>7</b>
2.1 Background .....	7
2.2 Flow Testing Capabilities for USHPRR.....	10
2.2.1 Hydro-Mechanical Flow Loop at the University of Missouri .....	10
2.2.2 Hydro-Mechanical Fuel Test Facility at the Oregon State University.....	11
2.2.3 Endurance Flow Loop at the Oregon State University .....	13
<b>3 Hydraulic Reactor Design Parameters .....</b>	<b>15</b>
3.1 Most Limiting Fuel Element Configuration in the Core.....	15
3.2 Summary of Design Parameters .....	18
3.3 Expected Behavior of the Plates .....	21
3.3.1 Critical Velocity Estimation .....	21
3.3.2 Expected Magnitude of Plate Deflections.....	22
<b>4 Initial Design and Conceptual Testing of Sensors .....</b>	<b>25</b>
4.1 Data Gathered and Its Purpose .....	25
4.1.1 Leading-edge Visualization.....	26
4.1.2 Deflection Measurements.....	27
4.1.3 Total Flow Rate and Individual Channel Flow Velocity Measurement.....	27
4.1.4 Pressure Drop Measurement Across the Entire Element.....	28
4.1.5 As-built Plate Thickness and Coolant Channel Profile Measurements .....	29
4.1.6 Summary .....	29
4.2 Sensors Previously Used at OSU .....	31
4.2.1 Sensors Used for Monitoring the Flow.....	31
4.2.1.1 Vortex Flow Meters.....	31
4.2.1.2 Differential and Static Pressure Instruments .....	31
4.2.1.3 Thermocouples .....	31

4.2.2	Strain Gauges.....	32
4.2.3	Fiber Optic Gauges.....	32
4.2.4	Pitot Tubes.....	33
4.2.5	Channel Gap Probe .....	34
4.2.6	Laser Surface Scanner.....	35
4.3	Proposed Sensors Requiring Testing.....	36
4.3.1	Laser Deflection Measurements .....	36
4.3.1.1	1-D Red Laser Spot Measurement.....	36
4.3.1.2	2-D Blue Laser Profile Measurement .....	37
4.3.2	Linear Variable Differential Transformers (LVDTs) .....	38
4.3.3	Inductive Sensor.....	38
4.3.4	Contact Sensor.....	39
4.4	Camera Systems.....	39
4.4.1	Machine Vision System.....	39
4.4.2	High-Speed Camera.....	40
4.5	Conceptual Design Sensor Testing Matrix .....	41
<b>5</b>	<b>Test Vehicle Design .....</b>	<b>45</b>
5.1	Test Vehicle Design Requirements.....	45
5.2	Conceptual Design of the Test Vehicle (Basket) .....	48
5.3	Element Constraints in the Test Vehicle .....	53
<b>6</b>	<b>Activities in Preparation for the Preliminary Flow Test Design .....</b>	<b>56</b>
6.1	Planned CFD and Structural Analyses of the Element in the Basket .....	56
6.2	Basket Fabrication for Fitting Purposes.....	57
6.3	Dummy Element Purchasing and Testing.....	57
<b>7</b>	<b>Summary.....</b>	<b>58</b>
	<b>References .....</b>	<b>60</b>
	<b>Acknowledgment .....</b>	<b>63</b>

# List of Figures

Figure 1.1. MITR reactor vessel cross-sectional view [1].	1
Figure 1.2. Isometric view of MITR LEU fuel element (left); cross-sectional view (right); T-plates are indicated in yellow, Y-plates in orange, and F-plates in red [4].	2
Figure 2.1. (a) The Hydro-Mechanical Flow Loop (HMFL) at the University of Missouri, and (b) schematics of the loop.	10
Figure 2.2. Hydro-Mechanical Fuel Test Facility at the Oregon State University (left); test section schematic (right).	12
Figure 2.3. The OSU Endurance Flow Loop (left); test-section schematic (right).	14
Figure 3.1. Cross-sectional view of MITR reactor vessel with various types of channels indicated. (Inset) most-limiting configuration of MITR elements, with two limiting plates highlighted.	16
Figure 3.2. Schematic of calculating combined coolant channel gap thickness: (a) nominal (side view), (b) conservative without lift (side view), (c) conservative with lift (top view). All dimensions in inch. Not drawn to scale.	17
Figure 3.3. Schematic of the MITR LEU element on the lower grid plate (in scale).	18
Figure 3.4. Plate displacement contour for nominal geometry and flow conditions.	22
Figure 3.5. Deflections of the MITR LEU plate due to FSI along the centerline.	24
Figure 4.1. A fully obstructed view of the outermost plates through the end fitting of the MITR LEU fuel element; from the top (left) at an angle (right).	27
Figure 4.2. A schematic of the inlet flow in the outer combined channel gap in MITR LEU core.	28
Figure 4.3. Flowmeter Layout.	31
Figure 4.4. Example Pitot tube plate from AFIP-7 (left) and close up of sensing end of tubes (right).	33
Figure 4.5. Example of Pitot tube installation in the instrumentation housing.	34
Figure 4.6. Example 3D printed (left) and wire-EDM (right) CGP guide blocks.	35
Figure 4.7. Laser surface scanner at OSU.	36
Figure 4.8. A schematic of Keyence LK-H152 laser measurement range.	37
Figure 4.9. A schematic of Keyence LJ-X8200 laser measurement range.	37
Figure 5.1. Isometric view of the basket with a porthole for displacement monitoring sensors.	48
Figure 5.2. Isometric view of the basket with a window for laser sensors.	49
Figure 5.3. Isometric view of the basket main shell.	49
Figure 5.4. Isometric view of the basket main shell and a groove for wiring.	50
Figure 5.5. Isometric view of the basket shell with a porthole for displacement monitoring sensors.	50
Figure 5.6. Isometric view of the basket shell with a window for laser sensors.	50
Figure 5.7. Isometric view of the basket end cap.	51
Figure 5.8. Installation of the basket in the instrumentation housing of the HMFTE.	51
Figure 5.9. Cross-section through a MITR LEU element installed in the testing basket.	52

Figure 5.10. Isometric view of a MITR LEU element installed in the testing basket with (left) and without (right) the end cap. ....52

Figure 5.11. Isometric view of the testing vehicle with potential locations of set screws for fuel element positioning.....54

Figure 5.12. Cross-section view of a MITR LEU element installed in the testing basket with the lateral constraints.....54

## List of Tables

Table 1.1. Comparison of geometrical characteristics of the MITR HEU and the MITR LEU fuel elements.....	3
Table 3.1. Channel gap thicknesses in the MITR LEU element.....	16
Table 3.2. MITR LEU hydraulic reactor design parameters for flow test.....	19
Table 3.3. Summary of the nominal and conservative flow rate per element. ....	20
Table 3.4. Comparison of velocity for one-element model and full-core model.....	20
Table 3.5. Miller’s critical velocity calculations for MITR LEU plate.....	22
Table 3.6. Description of selected cases in the FSI analysis [3]. ....	23
Table 4.1. Summary of test items and their purpose in the flow test.....	29
Table 4.2. Keyence LJ-X8200 measurement specifications.....	37
Table 4.3. PXIe-4340 LVDT sensor accuracy.....	38
Table 4.4. LVDT Physical Specifications.....	38
Table 4.5. Common resolutions and corresponding frame rates. ....	40
Table 4.6. Conceptual Design Sensor Testing Matrix. ....	42
Table 5.1. Design constraints for the flow test basket for the MITR LEU fuel element.....	45

# Acronyms and Abbreviations

Argonne	Argonne National Laboratory
CFD	Computational fluid dynamics
CGP	Channel gap probe
DDE	Design Demonstration Element
EFL	Endurance Flow Loop
F&RD	Functions and Requirements Document
FF	Fuel Fabrication
FQ	Fuel Qualification
FSI	Fluid-structure interaction
GTPA	Generic Test Plate Assembly
HEU	Highly enriched uranium
HMFL	Hydro-Mechanical Flow Loop
HMFTF	Hydro-Mechanical Fuel Test Facility
LEU	Low-enriched uranium
LSSS	Limiting Safety System Setting
LVDT	Linear variable differential transformer
M <sup>3</sup>	Office of Material Management and Minimization
MITR	Massachusetts Institute of Technology Reactor
MU	University of Missouri
MURR	University of Missouri Research Reactor
NNSA	U.S. National Nuclear Security Administration
NBSR	National Bureau of Standards Reactor
OSU	Oregon State University
RC	Reactor Conversion
SAR	Safety Analysis Report
U-10Mo	uranium-10 wt% molybdenum
USHPRR	U.S. High Performance Research Reactor

## Definition of Terms

Best estimate	Parameter value that is determined with the best available methods and/or models without including uncertainty.
Bounding	A parameter value that has been technically determined to not be exceeded under given conditions, such as, for example, normal operating conditions.
Conservative	Method, or resulting parameter value, that is not best estimate and includes uncertainty or margin whether discretionary or due to conservative assumptions.
Experiment design margin	The difference between an experiment target test value and a reactor design parameter value. The experiment design margin is increased (or decreased) on a discretionary basis or due to conservative assumptions.
Fuel core	The uranium-bearing region of each fuel plate.
Fuel foil	Metal uranium alloyed with molybdenum and bonded on the facing sides with zirconium diffusion barrier layers.
Fuel qualification	The process of designing, conducting, and evaluating experiments to ensure that the fuel is capable of performing without failure during reactor operations up to reported performance limits. Fuel qualification also includes measurements and reporting of fuel properties that can be used in performance and safety modeling.
Limiting safety system setting	Limiting values for settings of the safety channels by which point protective action must be initiated. The LSSSs are chosen so that automatic protective action terminates the abnormal situation before a safety limit is reached. The calculation of the LSSS shall include the process uncertainty, the overall measurement uncertainty, and transient phenomena of the process instrumentation.
Nominal	Value of a parameter under normal operating conditions.
Prototypic condition	Conditions that are considered representative of normal operating conditions and matching key aspects of the fuel design geometry.
Prototypic fuel	Fuel produced with a commercial-scale process consistent with the final specifications used for fabrication of fuel plates and elements.
Reactor design parameter	Best estimate value from reactor analysis used as a basis in experiment design for fuel qualification and licensing tests. Each reactor stakeholder in RC Pillar activities identifies and documents reactor design parameter values.
Regime appropriate	A set of conditions representative of reactor operations for which the value(s) does not have an impact on phenomena within a known range. For example, irradiation-induced creep in U-10Mo fuel at USHPRR operating conditions is not correlated to temperature, and therefore temperatures at which thermally induced creep does not occur can be referred to as “regime appropriate.”
Safety basis	A SAR, referenced supporting information, and other regulatory materials that provide the basis for safe operation of a reactor facility.
Safety margin	The difference between a regulatory limit and an appropriate value, that is either calculated or measured. Calculated values may include uncertainties to increase the conservatism of the safety margin.

---

Target test value	The goal value based on a reactor design parameter to be achieved during testing, such as during an irradiation experiment to support fuel qualification or fuel demonstration. The FQ, or other, Pillar identifies, and documents target test values in collaboration with other Pillars based on the reactor design parameters.
-------------------	-----------------------------------------------------------------------------------------------------------------------------------------------------------------------------------------------------------------------------------------------------------------------------------------------------------------------------------

# 1 Overview

## 1.1 Massachusetts Institute of Technology Reactor and Fuel Element

The Massachusetts Institute of Technology Reactor (MITR-II, also referred to as MITR) is a research reactor located in Cambridge, Massachusetts, designed primarily for experiments using neutron-beam and in-core irradiation facilities. Upgraded from MITR-I and relicensed as MITR-II, the MITR reactor has been in operation since 1975. It delivers neutron flux comparable to current LWR power reactors in a compact core with 6-MW licensed power using highly enriched uranium (HEU) dispersion fuel enriched at 93 wt%  $^{235}\text{U}$ . The Limiting Safety System Setting (LSSS) core flow rate is 1800 gpm. The reactor core is surrounded by a heavy-water reflector from the side and the bottom, and more than 10 ft of light water above the core region, which provide effective neutron shielding. All the fuel elements are of identical construction and have a rhomboid shape with internal angles of  $60^\circ$  and  $120^\circ$  [1]. As shown in Figure 1.1, the rhomboid elements are arranged in three concentric rings (A, B, and C rings) with three positions for the elements in the innermost ring, nine in the middle ring, and 15 in the outermost ring, for a total of 27 positions. These 27 positions are arranged so that the core has a hexagonal shape. There are boron-impregnated stainless-steel control blades along the hexagonal sides of the core. In the HEU core, typically, 24 of the 27 positions are occupied by fuel elements during normal operating conditions, and the other three are occupied by an in-core experimental facility or solid aluminum dummies.

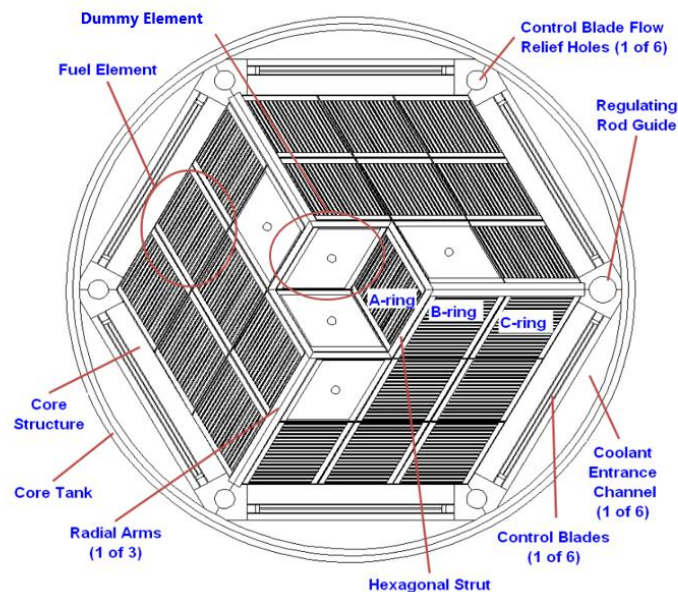
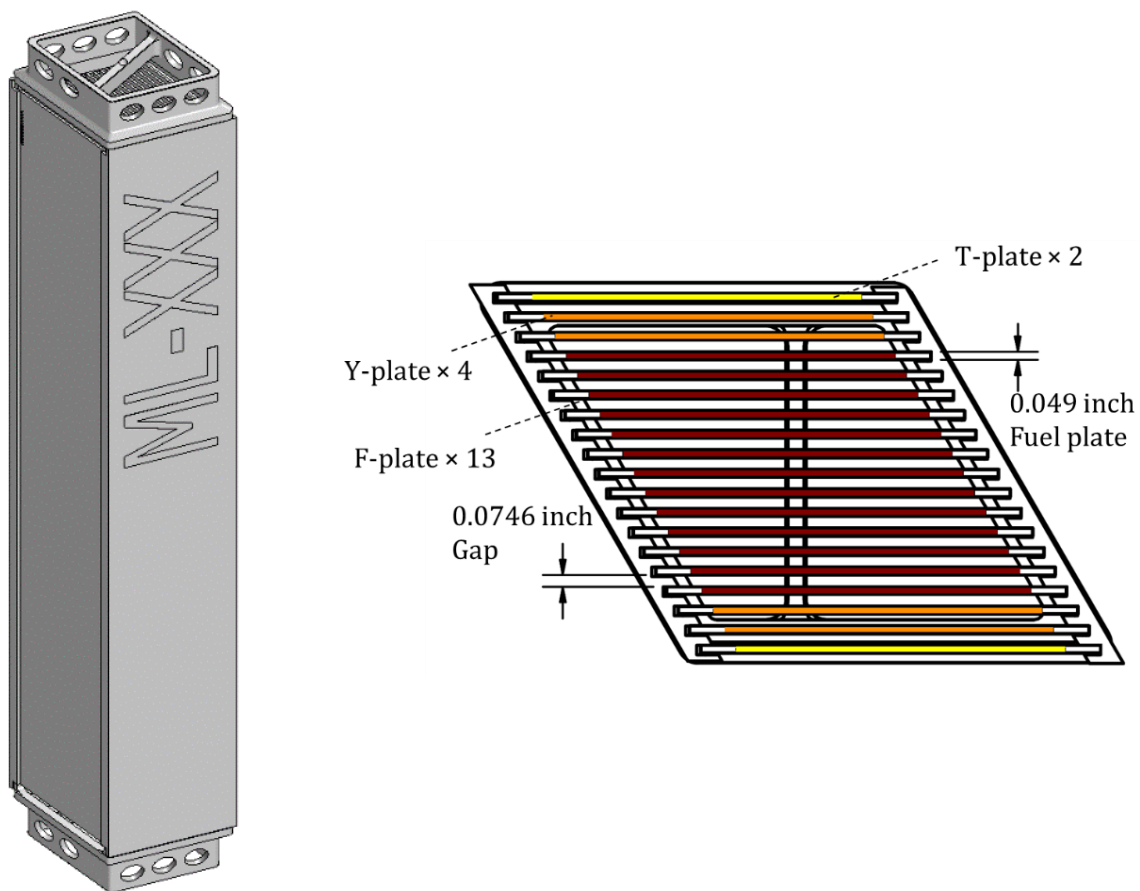


Figure 1.1. MITR reactor vessel cross-sectional view [1].

Each MITR HEU element has 15 fuel plates that are 23 inch long. The fuel core in each fuel plate is 22.375 inch long, 2.082 inch wide, and 0.030 inch thick. The aluminum cladding on each side of the core has a thickness of 0.015 inch. In addition, there are 110 external vertical aluminum fins extruded on the cladding of each fuel plate to enhance heat transfer. The fins are 0.010 inch apart, and each is

0.010 inch high and 0.010 inch wide. Thus, the distance from the fuel core surface to a fin root is 0.015 inch and to a fin tip is 0.025 inch. The center plate-to-center plate pitch is 0.158 inch, which implies that the fin-tip-to-fin-tip distance across the water channel between adjacent parallel fuel plates is 0.078 inch.

The MITR FYT low-enriched uranium (LEU) fuel element design has 19 finless fuel plates with a thickness of 0.049 inch per the 19B25 design in Bergeron, et al. [2]. The fuel core length and width, as well as the plate length and width are the same as in the HEU design. Reduction in the thickness of the plates reduces their bending rigidity [3]. Three different fuel core thicknesses were designed (F-full, Y-intermediate, T-thin) within the same overall plate thickness [4]. To minimize power peaking on the ends of the element, the fuel core thicknesses of the first three fuel plates from either end of the element have been made thinner than the 13 (0.025 inch thick) central plates ("F" type). The fuel plate ("T" type) at either end has a fuel-core thickness of 0.013 inch. The next two plates ("Y" type) from either end have core thicknesses of 0.017 inch. A 0.001-inch-thick zirconium interlayer is added on both sides of the fuel core. The cladding thickness is 0.011 inch, 0.015 inch, and 0.017 inch for F, Y, and T type plates, respectively. The water channel between interior plates is nominally 0.0746 inch thick. An isometric view of the proposed MITR LEU element and its cross-section schematic are shown in Figure 1.2. A comparison of geometrical characteristics of the MITR HEU and the MITR LEU fuel elements is listed in Table 1.1.



**Figure 1.2. Isometric view of MITR LEU fuel element (left); cross-sectional view (right); T-plates are indicated in yellow, Y-plates in orange, and F-plates in red [4].**

**Table 1.1. Comparison of geometrical characteristics of the MITR HEU and the MITR LEU fuel elements.**

	MITR HEU fuel element	MITR LEU fuel element
<b>Number of fuel plates</b>	15	19
<b>Interior channel thickness</b>	0.078 inch fin-tip-to-fin-tip	0.0746 inch
<b>Plate total thickness</b>	0.060 inch (0.080 inch with fins)	0.049 inch
<b>U-10Mo fuel core thickness</b>	0.030 inch	T plates (1, 19) – 0.013 inch, Y plates (2, 3, 17, 18) – 0.017 inch, F plates (4 to 16) – 0.025 inch
<b>Zirconium interlayer thickness</b>	-	0.001 inch
<b>AA6061 cladding thickness</b>	0.015 inch to the bottom of the groove, (0.025 inch to fin tip)	T plates (1, 19) – 0.017 inch, Y plates (2, 3, 17, 18) – 0.015 inch, F plates (4 to 16) – 0.011 inch
<b>Plate length</b>	23 inch	23 inch
<b>Length of the fueled region</b>	22.375 inch	22.375 inch
<b>Interior coolant channel width (between side plates)</b>	2.308 inch	2.308 inch

To maintain equivalent performance and experimental capabilities of the reactor facility with the LEU fuel design, the power of the proposed LEU core was increased to 7 MW, which is 1 MW higher than that of the HEU core. To maintain safe temperature levels in the core and in the cladding and especially on its surface, the primary coolant flow rate for the LEU cores has been increased by 20% as compared to the HEU core, from 2000 gpm to 2400 gpm. The LSSS flow rate for the proposed LEU core is 2200 gpm, which is 400 gpm greater than that for the HEU core. Further details on the LEU element design and comparison with the HEU fuel element can be found in [2] and [5].

The HEU fuel elements have been operating within the MITR for several decades with an excellent performance history. Experiments conducted during the design and original start-up stages did not indicate any visible oscillations of the plates [6]. However, the proposed MITR LEU fuel plates are thinner than the HEU plates and do not have fins, and therefore have a reduced bending stiffness as compared to the HEU plates [3]. The changes in the plates' geometry and the increased flow rate, create less favorable conditions for the MITR LEU fuel plates from the perspective of the hydrodynamic stability as compared to the conditions for the MITR HEU fuel plates. Thus, flow test and the supporting computational fluid dynamics (CFD) analyses are warranted in the preparation for licensing of the MITR LEU fuel element designs.

## 1.2 Functions and Requirements for the LEU Fuel Elements

The USHPRR Functions and Requirements (F&R) Document [7] has been issued to document the functions and requirements of the new LEU fuel systems that the U.S. High Performance Research Reactors (USHPRR) Project is developing for the conversion of the USHPRR from HEU. The functions identify what the fuel systems should do, and the requirements define the parameters for performing these functions. The F&RD also describes the key performance attributes that guide the development of the fuel and fabrication processes as a component of the requirements. Below, several of these requirements warranting the flow test are outlined.

Under function F 1.1 “Maintain Mechanical Integrity”, the following requirements, among others, are listed:

- R 1.1.2. The mechanical response of the fuel core, cladding, and any interlayers or other fuel plate components during normal operations and transients where fuel integrity is required shall be established. (Basis: NUREG-1537, Part 1, Chapter 18 and Chapter 4 section 4.2.1. Retention of fission products capability and establishment of safety limits.)
- R 1.1.3. The fuel element shall not fail mechanically during normal operations and transients where fuel integrity is required. (Basis: NUREG-1537, Section 4.2.1, Maintain fission products and integrity of fuel element.)

Under function F 1.2 “Maintain Geometric Stability,” the following requirements, among others, are listed:

- R 1.2.3. Fuel performance and structural stability shall be maintained so that reactor coolant flow keeps fuel plate heat transfer and/or temperatures within the reactor safety analysis envelope (Basis: The ability to cool the reactor fuel must be maintained. Report ANL/RERTR/TM-11-28 on flow instability model for MURR states flow instability avoidance as a safety requirement for MURR.)
- R 1.2.4. Plate movement caused by pressure differential shall not compromise ability to cool the fuel. (Basis: Geometry of the fuel must be stable and predictable to maintain cooling.)
- R 1.2.5. Changes in channel gap shall not compromise ability to cool the fuel. (Basis: Ability to cool the fuel during normal and transient conditions must be maintained allowing for geometry changes [volumetric swelling, twist, thermal expansion, and deflection, etc.] )

Under function F 1.5 “Test to Verify Design Requirements Have Been Met,” the following requirements, among others, are listed:

- R 1.5.1. Verification (i.e., tests, reviews, analyses) shall be completed to demonstrate that the fuel elements are designed to accommodate expected mechanical forces and stresses, hydraulic forces, thermal changes and temperature gradients, internal pressures including that from fission products and gas evolution, and radiation effects including the maximum fission densities, fission rates, and fuel temperatures. (Basis: NUREG-1537, Part 1, section 4.2.1.)

## 1.3 Flow Test Goal

The experimental needs for qualification of the proposed design of the LEU fuel elements consist of two major components conducted at the full element level: the hydraulic performance evaluation led by the Rector Conversion (RC) Pillar and the irradiation testing led by the Fuel Qualification (FQ) Pillar.

The purpose of the hydraulic performance evaluation of the MITR LEU fuel element designed by the RC Pillar is to test a prototypic commercially fabricated LEU fuel element, to determine whether any failure modes are observed in the fuel element, including significant deformations such as plate bending, twisting, or plate detachment from the side plate under selected safety basis limits for reactor flow conditions. The evaluation will be performed by a combination of out-of-pile flow test and supporting analyses. Although margins to these failure modes need to be present, the tests are not meant to be run to failure (loss of integrity or large deflections) of the fuel elements. To demonstrate the existence of such margins, the most conservative MITR core configuration (in terms of the number of fuel elements in the core and their orientation) will be considered. In addition, the flow rates during the test will be increased beyond the normal operation band. That core configuration and the conservative flow conditions (from the perspective of flow-induced deflections) are described in Section 2 of this report.

Another component of the hydraulic performance evaluation of the MITR LEU fuel element design includes computational analyses (both CFD and fluid-structure interaction [FSI]) that are meant to guide certain aspects of the tests (e.g., instrumentation placement) and provide data that are complementary to the experimental observations (e.g., sensitivity study).

It is noted that separate flow test will be performed within the USHPRR Project as part of the MITR Design Demonstration Element (DDE) irradiation test led by the FQ Pillar. The MITR DDE will be irradiated in a non-native test reactor (BR2) under irradiation conditions designed to be as prototypic of the MITR LEU fuel element as possible. While the irradiation test contains an aspect of flow test, the MITR DDE end fittings have a significantly modified shape. Hence, the flow conditions in these tests (as close to nominal as practical) will not be representative of the most conservative configuration from the perspective of the hydro-mechanical stability of the fuel elements.

## 1.4 Flow Test Conceptual Design Goal

The first technical objective of the flow test conceptual design is to perform a review of the hydraulic reactor design parameters of MITR to represent best estimate values and account for uncertainties that may lead to more conservative values in MITR LEU core. As a part of this, there is also an evaluation of adequate additional experiment design margin which includes differences between the reactor core and the flow test. In order to initially analyze these systems, a flow network analysis with both a reactor core and a single element in the basket was performed. Confirmatory CFD and FSI analyses are to be performed during the preliminary stage following the proposed plan given in Section 6.1 of this report.

The second technical objective is to review the methods and sensors for monitoring various hydraulic and mechanical characteristics of the flow test. Testing the sensors by Oregon State University (OSU)

on a single plate and an all-aluminum mockup of the MITR LEU fuel element are planned for the preliminary and the final stages of the flow test design, respectively.

The maximum static deflections of fuel plates in MITR LEU elements caused by a pressure differential in the channel gaps are expected to be in the range of 2 mil (1 mil = 0.001 inch) based on preliminary numerical analyses (see Section 3.3 and [3] for details). Since such small deflections are difficult to measure in fuel plates under the flow conditions, the quantification of the total deflections is desired but not required to achieve a successful flow test. Quantification of the plastic (permanent) deformations in the fuel element is required via the analysis of pre-test (as-built), and post-test geometry (see Section 4.2.5 for permanent deflections measurement). Techniques for visualization, and measurements of the deflections of the plate's leading edge (where the deflections in the MITR LEU fuel element are expected to be the largest) are of interest at the current conceptual stage of the flow test. As an alternative, a confirmation that the deflections are below the known accuracy of a measuring device is sufficient. In such a case, the confirmed uncertainty of the measurement must be shown to be of a similar scale as the expected maximum deflection of the MITR LEU fuel plate under the hydrodynamic load (see Section 3.3 for the determination of that value).

The third technical objective of this work is to develop a conceptual design of a testing vehicle (basket) that will accommodate the prototypic MITR LEU elements in the Hydro-Mechanical Fuel Test Facility (HMFTF) flow loop for hydro-mechanical testing. The outer dimensions of the basket must allow for insertion to the test section of the HMFTF flow loop. The internal dimensions of the basket should represent the most limiting configuration in the core. The geometrical features of the basket must be machinable with the techniques and equipment available at Argonne National Laboratory (Argonne). The conceptual design of the basket and the evaluation of the sensors will take into consideration the accessibility of the most limiting plate in the MITR LEU element. The basket also needs to be structurally sound enough not to deform during handling, assembly, and flow test.

The flow test conceptual design will also focus on other preparatory tasks for the later stages of the flow test design, including planning for supporting numerical analyses, procurement of the sensors, and purchase of dummy elements for sensor testing.

## 2 Experimental Methods

### 2.1 Background

The original design work on U.S. research reactors was conducted in the late 1940s through the 1960s. The early experiments conducted at Oak Ridge National Laboratory by Stromquist and Sisman in 1948 indicated that, at sufficiently high flow velocities, mockup flat plates were deforming plastically, and curved plates experienced a reversal of curvature (i.e., were buckling) [8]. These deformations were caused by pressure differential on the two sides of the plate due to the imbalance of the flow. As a result, one or more channels in the assembly were completely closed. A vibrometer was used to monitor the vibrations of the plates using six pins inserted into the testing section via small ports.

The phenomenon of plate collapse observed by Stromquist and Sisman raised a concern and triggered a series of experiments and analyses conducted in later years by many researchers. The most often cited of these was Miller, who in 1958 derived formulas for critical coolant velocity at which elastic plates can lose their stability and collapse [9]. Miller derived his equations for both initially flat and curved plates with a multitude of boundary conditions including built-in (fixed) and hinged (simply supported) plates (see Section 3.3.1 for details).

Many researchers have continued the work begun by Miller. Some of the results, especially those coming from the theoretical derivations, supported Miller's findings. However, a substantial group of experimental studies did not confirm the presence of the critical velocity that would mark the onset of instabilities or collapse. Instead, they reported gradually increasing deflections of the plates and/or vibrations, depending on the flow conditions.

Refinements of Miller's theory came from, among others, Johansson [10]. One of Miller's original assumptions was that all channels have an equal thickness. He also assumed that the length of the plate is significantly larger than the length of the deflected region. By using wide beam theory to describe the deflection of the plates, he neglected the three-dimensional character of the deflections. In Miller's derivation, the friction pressure drop in the deflected region is small, and inertia effects in the fluid are ignored. In his work, Johansson made corrections to some of these assumptions. He accounted for flow redistribution between adjacent channels due to the plate's deflection. This caused further pressure increment acting on the plate. Also, by including axial bending in the analysis, the three-dimensional character of the deflection region was accounted for. Depending on the geometrical aspects of the plates, he predicted critical coolant velocity to be between 0.8 and 1.6 times that of Miller. He concluded that the addition of comb support at the leading edge locally increases the critical velocity significantly and moves the most critical region in the plate from the leading edge to about one to two spans of the plate between the supports downstream from the leading edge.

In 1962 Rosenberg and Youngdahl [11] included inertia effects in their analysis and formulated a dynamic model of the plate stability in the coolant flow. Their model confirmed Miller's finding of the presence of divergence (deflections increasing with time) at higher velocities and stable oscillations at lower velocities. Further improvements of Miller's theory were made, among others,

by Scavuzzo (1965) who coupled the hydraulic equations with the plate equations to obtain non-linear integral equations describing the plate's deflection even more accurately [12].

In the late 1950s, Zabriskie studied the deflection of single and multiple plate assemblies with and without leading-edge support combs [13], relating his findings to those reported by Miller. A sudden collapse was not observed in these experiments. Instead, in all conducted tests, the deflections grew progressively with increasing velocity. However, agreement within 20% of Miller's theory was reported for most of the cases. Zabriskie used pressure taps installed along the plate axis in the side plates to characterize the pressure differentials acting on the plates. He subsequently utilized simple beam theory to correlate these pressure differentials to the deflection of the plates. The presence of the combs on the leading edge increased the stability of aluminum plates allowing for higher flow velocities.

In 1963 Groninger and Kane tested three 5-plate assemblies to examine their deflections due to the parallel flow [14]. The experiments introduced specially designed strain gauges embedded in the plate edges to measure the deflections indirectly. Flow velocities up to 190% of Miller's critical velocity were considered in these tests. The primary conclusion of this work was that the critical velocity deflection is a magnification of the initial perturbations in the fuel plates. The authors did not observe catastrophic or sudden deformations of the plates. They noticed that the adjacent plates always deform in opposite directions at high flow rates, either opening or closing the channels. High-frequency vibrations (flutter) were noticed for the highest flow velocities. The comb installed on the leading edge suppressed this behavior, but large deformations were still present away from the leading edge. Further theoretical analysis performed by Kane [15] also focused on the influence of initial imperfections in the plate geometry near the leading edge on the increase in the flow-induced deflections. Kane concluded that small differences in channel gap thickness for flow rates near the Miller's critical velocity exacerbate the deflections.

In 1968 Smissaert conducted a set of experiments on plate assemblies made of PVC to characterize the static and dynamic behavior of the plates at different flow velocities [16]. Five-, nine-, and fifteen-plate assemblies were investigated. Strain gauges were embedded along the center plate's length in the middle of the span to capture the entire profile of the deflected plate. Because of the minimum thickness needed for the installation of the pressure taps, only the assembly with the largest channel gaps (the five-plate assembly) was instrumented with them. The maximum flow rates in the test reached 3.5 times Miller's critical velocity. Smissaert identified several instabilities in the plate: static deflection of the leading edge, static deflection over the full length of the plates in the plate array, small amplitude traveling waves, and large amplitude flutter. He noticed that for low velocities, the plates deformed as a result of a static pressure differential in the channels. The flutter, consisting of traveling waves, originated at the leading edge of the plate and ran down the plate in the direction of the flow. The wavelength of the deformation was a function of the coolant velocity. High-frequency flutter instabilities, without sudden collapse, were reported for velocities close to two times Miller's critical velocity. These tests also showed that any disturbance of flow entering the channels surrounding the fuel plates has a significant effect on plate deflections. Smissaert also noticed that installing a support comb on the leading edge suppresses the high-frequency flutter and significantly reduces the deflections in the plates.

In the early 1990s Swinson, et al. conducted flow tests on involute plate assemblies in support of the Advanced Neutron Source reactor design [17], [18], [19], [20]. To lower the flow velocity and pressure required for the anticipated collapse conditions, the test assemblies were constructed of epoxy. Five-plate assemblies were the subject of the experiments. Each of the inner three plates in the assembly

was instrumented with five strain gauges placed along the center axis. The gauges were located near the leading edge, at 25%, 50%, and 75% of the plate's length, and near the trailing edge. Five static pressure taps in each channel were positioned in the same cross-sectional plane as the strain gauges. The maximum deflections were measured either at the leading edge or at a three-quarter length of the plate. The author formulated an analytical solution for the maximum involute plate deflection due to a pressure load using Castigliano's energy theorems for deformation. The deflections calculated through this analytical approach were compared with the deflections experimentally found with the strain gauges. The calculated values were a reasonable approximation of the measured values.

In 2004 Ho, et al. performed a series of experiments on two-plate assemblies in order to support the design of the Replacement Research Reactor for the Australian Nuclear Science and Technology Organisation (ANSTO) [21]. The plates were instrumented with strain gauges at three positions: the leading edge, the middle of the plate, and the trailing edge. At each position, two strain gauges were installed on either side of the plate. To prevent the strain gauges from influencing the flow in thin channels, the gauges were epoxied into a groove milled on the plate's surface. The results show plate collapse occurring at an average velocity of 78% of Miller's critical velocity. During the plate collapse, cavitation was observed on the leading edge of the deformed plate. The mode of collapse in these experiments appeared to be random, with both plates collapsing onto each other or both deflecting away from each other.

In early 2010's Liu et al. [22] and Li et al. [23] performed a study on FSI for single and double plate assemblies in water flow. In their experiments, Liu, et al. constrained only the four corners of the plates, which significantly increased the deflection of the plates as compared to the plates constrained along two long edges. The testing section was enclosed with Plexiglas, which allowed for the utilization of a laser sensor for the measurement of the plate's deflection. Li, et al. found several regimes of flow rates that resulted in different characteristic responses. At the lowest velocities, the thickness of the channel between the plates was reduced, and no vibrations were present. At higher velocities, large vibrations occurred, causing both plates to oscillate in the same or opposite phases, depending on the flow rate regime.

In 2017, Castro et al. [24] reported on experiments conducted on two-plate assemblies with dimensions similar to those in the fuel element of the Brazilian Multipurpose Reactor. The aluminum plates were enclosed in a testing section made of Plexiglas. Strain gauges were installed near the inlet, the middle, and the trailing edge of the plate to indirectly measure the deflections. Pressure drop measurements were used as a secondary method for detecting the collapse of the plates. Collapse and plastic deformations of the plates were reported at flow velocity close to 85.5% of Miller's critical velocity. Below that velocity, the maximum deflection on the leading edge was proportional to the squared velocity.

Past experiments mentioned in this section remain an important reference in this evaluation of fuel plate hydro-mechanical performance, both in terms of designing fuel plate assemblies and in informing the selection of measurement techniques. Most of the described experiments made use of the strain gauges installed on the surface of the plate to measure the deflections. This technique was proven to work for the detection of static deflections as well as dynamic flutter. However, these experiments were mostly focused on characterizing the response of the plates to coolant flow rates reaching, or exceeding, Miller's critical velocity. In contrast, the flow tests for the USHPRR LEU fuel elements will be executed at significantly lower flow rates which are a fraction of Miller's critical velocity (see Section 3.2). Also, the deflections of the plates are expected to be at the level of a fraction of the MITR LEU element channel gap thickness (see Section 3.3). Thus, the conceptual design of the

flow test is focusing on selecting the most appropriate sensors that can detect the expected deflections in the plates under the nominal and conservative MITR conditions.

## 2.2 Flow Testing Capabilities for USHPRR

To support the evaluation of the hydraulic performance of the USHPRR LEU fuel elements, the USHPRR Project commissioned the development of two experimental facilities: the Hydro-Mechanical Flow Loop (HMFL) at the University of Missouri (MU) and the HMFTF at OSU. Both facilities have hosted a series of flow test experiments in previous testing campaigns; the outcomes of these testing efforts have resulted in an impact on the design of the current flow tests. The following sections briefly describe these two facilities and some of the experiments performed there.

### 2.2.1 Hydro-Mechanical Flow Loop at the University of Missouri

Initial work for the RC Pillar's hydraulic performance evaluation of the LEU fuel elements has been performed at the HMFL at MU. The flow loop and a flow path schematic of HMFL are shown in parts a and b, respectively, of Figure 2.1. This flow loop includes a National Instruments cDAQ system for data collection and control of the flow. User control and monitoring are accomplished with LabView software.

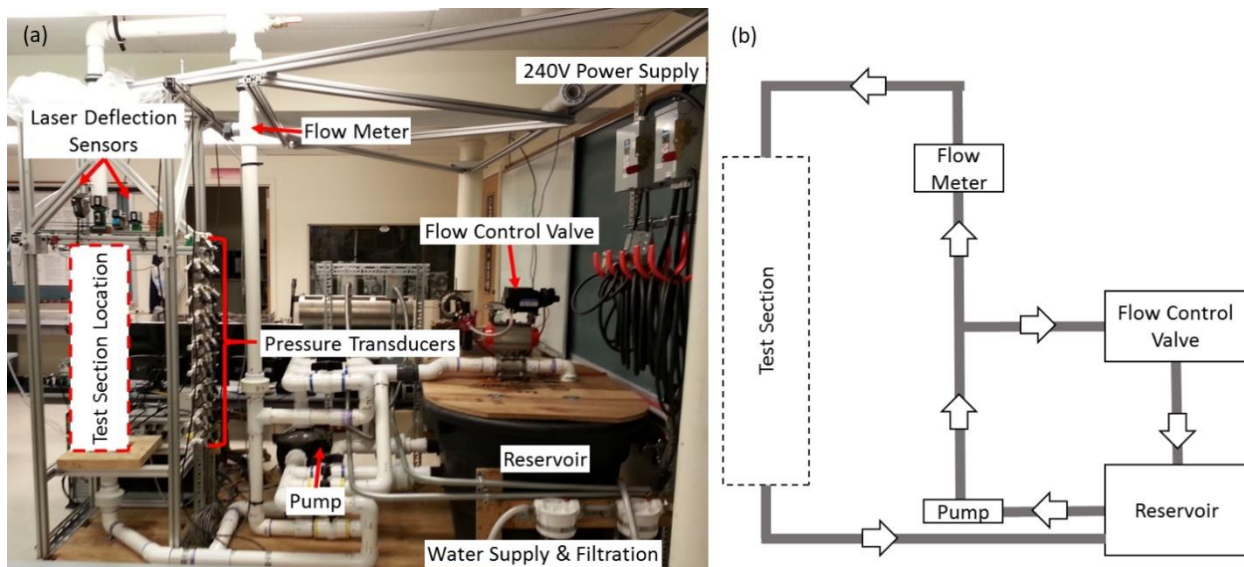


**Figure 2.1. (a) The Hydro-Mechanical Flow Loop (HMFL) at the University of Missouri, and (b) schematics of the loop.**

The water flow loop was designed to accommodate a wide range of test sections. So far, single flat and cylindrical aluminum plates with two surrounding channels have been tested at the facility at varying flow rates [25]. During the tests, the pressure differential between the two fluid channels was monitored with the use of Omega PX-26 differential pressure transducers. The total flow rate was measured with an in-line flow meter. To map the thickness of the fluid channels and monitor plate deflection during the flow test, two Keyence LK-G152 laser displacement sensors were used.

The test sections were built with a wider channel gap on one side of the test plate and a narrower channel gap on the other side. This represents the differences that could be encountered in USHPRR LEU fuel elements due to allowed fabrication tolerances. The flat plate was nominally 0.040 inch thick. The outer walls of the channels in the flat plate experiments were built of transparent plexiglass to allow for the mapping of the channel gap thicknesses with the motor-operated laser sensor. The laser was also used for monitoring the deflection of the plate at several locations along the centerline of the plate. The variation in the channel gap thickness was a combination of the plate shape and the channel's wall imperfections. Sizeable imperfections that were detected before the test influenced the magnitude and the shape of the plate's deflections. The maximum displacements occurred at the leading edge of the plate with similar magnitude deflections near the middle of the plate in the axial direction.

Numerical models of the setup were built with the use of STAR-CCM+ software to study the behavior of the plate as a FSI problem. Pre-deforming the modeled plate, using the distribution of the mapped imperfections of the channel gap thickness, allowed for obtaining results that closely matched the experimental data.

In the curved plate experiments, the outer channel walls were built of stainless-steel cylinders. The cylindrical plate was built of a 0.0159-inch-thick sheet of aluminum. In this case, the majority of the imperfections in the channel gap thickness came from the shape and the position of the tested plate between the inner and outer cylinders. Since the mapping could not be done with a laser through the opaque walls, a depth micrometer was used to measure the variation in the channel gap thickness. The displacements of the plate were measured again with the use of the laser, but only through a series of five plexiglass windows installed in the outer cylinder. Again, after including the measured imperfections in the position and flatness of the plate in the numerical models of the setup, a close match between the simulations and the experiments was found.

These experiments have proven that laser sensors can resolve small deflections of the plates (around 4 mil) with a reasonable level of uncertainty (~1 mil). Also, they have confirmed that information about the as-built geometry is required for the numerical models to match the experimental data.

## **2.2.2 Hydro-Mechanical Fuel Test Facility at the Oregon State University**

The HMFTF (see Figure 2.2) is located in the Advanced Nuclear Systems Engineering Laboratory at OSU [26], [27], [28]. It is a large-scale thermal-hydraulic separate-effects test facility operating in conformance with the American Society of Mechanical Engineers (ASME) Nuclear Quality Assurance (NQA-1) standard (ASME NQA-1-2008 with 2009 Addenda) [29]. The facility allows for testing a wide range of elements, provided that they fit into the 15-foot-tall test section. Test section diameter is that of 6-inch Schedule 40 stainless steel (SCH40S) pipe with nominal internal diameter of 6.065 inch. The HMFTF facility was designed to envelop the flow rate, temperature, and pressure operating conditions of all high performance research reactors in the U.S., as well as those conditions required for fuel qualification. The operating range of the loop covers flow rates ranging from 100 gpm to 1600 gpm. The testing loop is rated to 600 psig and 460 °F. The configuration of the loop allows for upward and downward flows through the test section.



**Figure 2.2. Hydro-Mechanical Fuel Test Facility at the Oregon State University (left); test section schematic (right).**

To date, multiple experiments have been performed at HMFTF supporting FQ Pillar's efforts, including the MP-1, EMPIRE, FSP-1, AFIP-7 [30], and Generic Test Plate Assembly (GTPA) campaigns. The recently published results of the GTPA experiments document many findings that are instrumental to the entire conversion effort, including experience with the sensors and methodology for monitoring the structural response of thin fuel plates to hydrodynamic load induced by coolant flowing through dissimilar channel gaps [31], [32].

The GTPA compared the response of plates made of four different compositions:

1. A homogenous hot and cold rolled AA6061-T6,
2. DU-Monolithic foil plate,
3. SS-Dispersion fuel plate, and
4. A homogenous sheet AA6061-O.

Each plate was tested within an assembly totaling six plates, with five of them significantly more resistant to bending (comprising Hastelloy HX alloy) than the tested plate. The tested plates were 0.050 inch thick with a nominal channel gap thickness in the assembly of 0.075 inch and one channel gap approximately 0.188 inch thick, creating a pressure differential acting on the tested plate.

In the experiment, standard strain gauges (providing point data), as well as fiber optic-based LUNA gauges (providing linear data), were used to monitor strains and hence deflections in the plates. While able to provide high-frequency data, the standard strain gauges were not suitable for monitoring low-magnitude deflections of the plates because of high noise in the recorded output

under the flow conditions during the GTPA tests (high flow rate, pressure, and temperature) [32], [31]. However, they were useful in exploring the dynamic response of individual plates within an element both during steady and transient flow conditions (see Section 4.2 for more information).

The GTPA experiments have shown that all tested plates responded similarly in the elastic range of the responses (i.e., had similar bending stiffness). AA6061-O is a conservative material choice for predicting the hydro-mechanical responses of plate-type fuels as it was the first one to collapse at high flow rates. Gradually increasing plate deformations were not observed with increasing flow rate. On the contrary, a sudden collapse of the plates has been noted for all failed plates.

Because of its versatility, NQA-1 compliance, and ability to handle USHPRR LEU fuel elements, OSU HMFTF was chosen to conduct the shakedown flow test for MITR LEU fuel element described in this report.

### **2.2.3 Endurance Flow Loop at the Oregon State University**

Besides the HMFTF, OSU also operates several testing flow loops used for studying separate effects in plate-type fuel elements; one of these is the Endurance Flow Loop (EFL). The EFL is a parallel-system welded stainless steel flow loop designed to force a controlled volumetric rate of water over mock-up reactor fuel plates to simulate in-pile hydraulic conditions. Although compact in size, the EFL is outfitted with several different flow paths balanced by strategically placed valves to divert flow, enabling desired flow and pressure conditions to be achieved with respect to the fuel elements (see Figure 2.3). All hardware and sensors on the EFL are controlled or monitored through a Data Acquisition System and displayed in a Graphical User Interface control panel on the computer [33].

The driving force for the flow in the EFL is a twin-stage 10-hp vertical in-line pump that can deliver 35 to 225 gpm and provide a differential pressure of up to 200 ft dynamic head. This pump is controlled via a variable speed drive which adjusts the rotational speed of the pump. The flow through the EFL is measured from three vortex-style Rosemount flow meters, which cover the whole operational range of the system. Pressure transmitters are placed around the facility to monitor the gauge pressure of the inlet test sections and the differential pressure across the fuel elements and the pump. Three thermocouples are located on the facility to measure the bulk coolant temperature and the differential temperature across the pump. Water quality is measured by pH and conductivity probes. The EFL is limited to a pressure of about 150 psig, and a temperature of 200 °F enveloping the flow conditions of the MITR.

A portion of the preparatory tests, including a feasibility study and demonstration of the sensors, is planned to be performed at the EFL facility. The capabilities of this facility are sufficient to perform the relevant flow tests with a significantly shorter turnaround time as compared to the large-scale HMFTF loop.

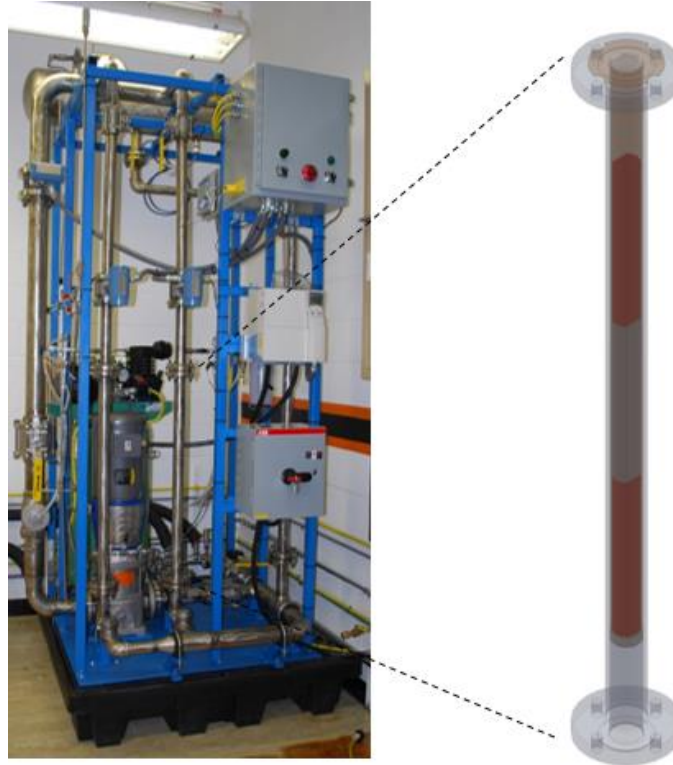


**Figure 2.3. The OSU Endurance Flow Loop (left); test-section schematic (right).**

## 3 Hydraulic Reactor Design Parameters

### 3.1 Most Limiting Fuel Element Configuration in the Core

From the structural mechanics perspective, all plates in the MITR LEU element have almost identical bending stiffness (as confirmed in [3], and by the three-point bending experiments that supported the GTPA testing performed at OSU [32], [31]). Marginal differences come from different thicknesses of the fuel core, which has a slightly higher Young's modulus than the AA6061 cladding. Thus, the magnitude of the plates' deflection is mainly governed by the magnitude of a pressure differential acting on them. Due to the nonuniform channel thicknesses and flow conditions around the elements, the pressure differential acting on each of the fuel plates is not the same for all the plates in the MITR core. For these reasons, the position of the plate in the element and the core influences the magnitude of the flow-induced deflections. The most limiting plate in the core, from the perspective of coolant flow-induced deflection, can be determined by analyzing the orientation of the LEU elements in the core.

Figure 3.1 shows the cross-section of the MITR core, with various types of channels indicated. The design of the reactor and the fuel elements allows for various orientations of the elements in the core and the one shown in the figure is just an example of the possible scenarios. The end channel gaps of each fuel element may face the core structure, or another fuel element facing it with its side plate, or another outer channel. In the case in which the end channels of two neighboring elements face each other (case (a) or (b) in Figure 3.1), they form a combined coolant channel gap with a thickness about twice the thickness of an internal channel gap. It must be noted that typical core configurations will not have two fuel elements in A-ring, as two of the three locations of A-ring are usually occupied by solid dummy elements. Therefore, the combined end channel is less likely to appear in A-ring and only the configuration (b) is likely to occur in the core. Granted, the combined end channel is not completely sealed between the two elements, but the flow outside of the element is significantly constricted. Thus, for conservatism and simplification of calculations and testing, it may be assumed that this is a single combined channel. Such configuration leads to the largest disparity in the channel thicknesses, flow rates, and pressure differentials on the two sides of the external plates in the fuel element. The most limiting plates resulting from that configuration of elements in the core are shown in yellow in Figure 3.1. The design of the testing vehicle (basket) for the MITR LEU fuel element must focus on recreating these geometrical conditions for the outermost plate of the tested element.

The most relevant geometry aspects of the MITR LEU fuel element were determined through a review of the technical drawings [34], [35], [36], [37] of the MITR LEU fuel element and are presented in [38]. Table 3.1 lists the possible theoretical channel gap thicknesses within the MITR LEU fuel element for the (b) configuration of the fuel elements in the core (see Figure 3.1). The fuel element used in the flow test will be produced to meet the specifications of the MITR LEU element with no additional modifications for testing purposes. Thus, the internal dimensions (including channel gap thicknesses) will not be controlled in the test. However, it is planned that the design of the basket will allow control (within a limited range) of the thickness of the outer channel gap thickness. To meet the goal of the flow test, the most conservative conditions for the outer channel gap thickness must be established and will be targeted in the flow test.

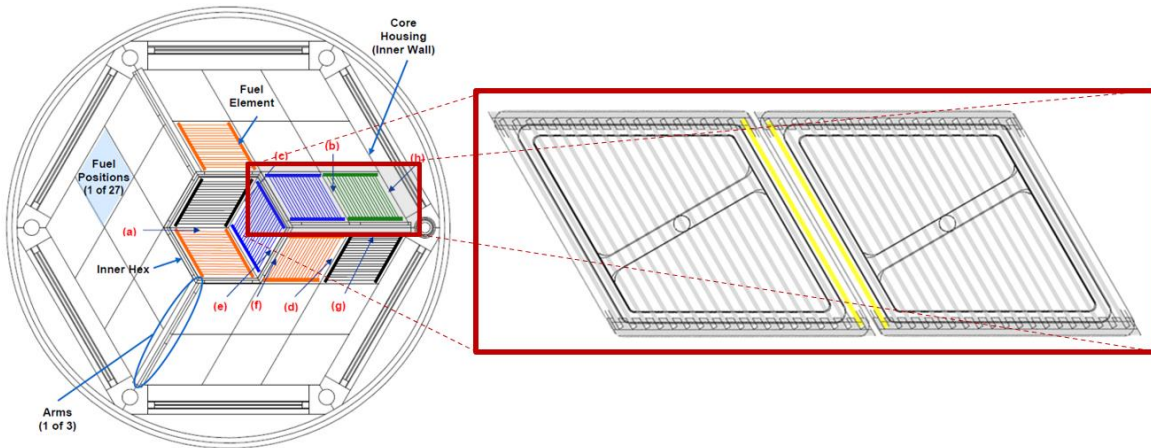


**Figure 3.1. Cross-sectional view of MITR reactor vessel with various types of channels indicated. (Inset) most-limiting configuration of MITR elements, with two limiting plates highlighted.**

The nominal size for the combined end channel gap ((b) in Figure 3.1) was determined to be 0.141 inch, as shown in Figure 3.2 (a). When the fabrication tolerances of the end fitting of the fuel element are considered, the largest possible channel gap thickness may be as large as 0.186 inch, as shown in the schematic drawing in Figure 3.2 (b). Furthermore, since the MITR fuel element is positioned in the lower grid plate without any mechanical constraints that could prevent limited movement of the element in the axial direction, the fuel element can be lifted by the hydrodynamic forces exerted by the upward flow of the coolant (see Figure 3.3 for a schematic of that geometry, refer to Appendix A of [3] for the lift-up force calculations). The magnitude of that motion is limited by the presence of the upper grid. Because of the chamfered design of the end fitting, axial motion creates a possibility for further increase of the outer channel gap thickness up to 0.247 inch in the worst-case scenario, as shown in the schematic drawing in Figure 3.2 (c). Since a larger channel gap thickness disparity will result in a larger velocity disparity and fuel plate displacement, the largest outer channel gap thickness will be used as the design requirement for the testing vehicle. Note that the 0.247 inch of combined end channel gap thickness is very conservative by assuming that all tolerances accumulate in the adverse way, and the probability of forming a combined end channel with 0.247 inch in the MITR core is very low. In addition, the full core flow network analysis shows that the internal channel flow velocity/rate reduces only 0.7% if increasing the thickness of a combined end channel in the core from 0.141 inch to 0.247 inch, indicating that the effect of an end channel with such a conservative thickness (0.247 inch) on the flow rate (and cooling capability) of internal channels is negligible. This can be calculated from the velocity data in Table 4.2 of Wang et al. [3].

**Table 3.1. Channel gap thicknesses in the MITR LEU element.**

Geometry category	Size (inch)	Note
Nominal internal channel gap thickness	0.0746	The thinnest within tolerances is 0.070 inch
Combined end channel 1 gap thickness	0.141	Nominal
Combined end channel 2 gap thickness	0.186	Conservative without lift
<b>Combined end channel 3 gap thickness</b>	<b>0.247</b>	<b>Conservative with lift</b>

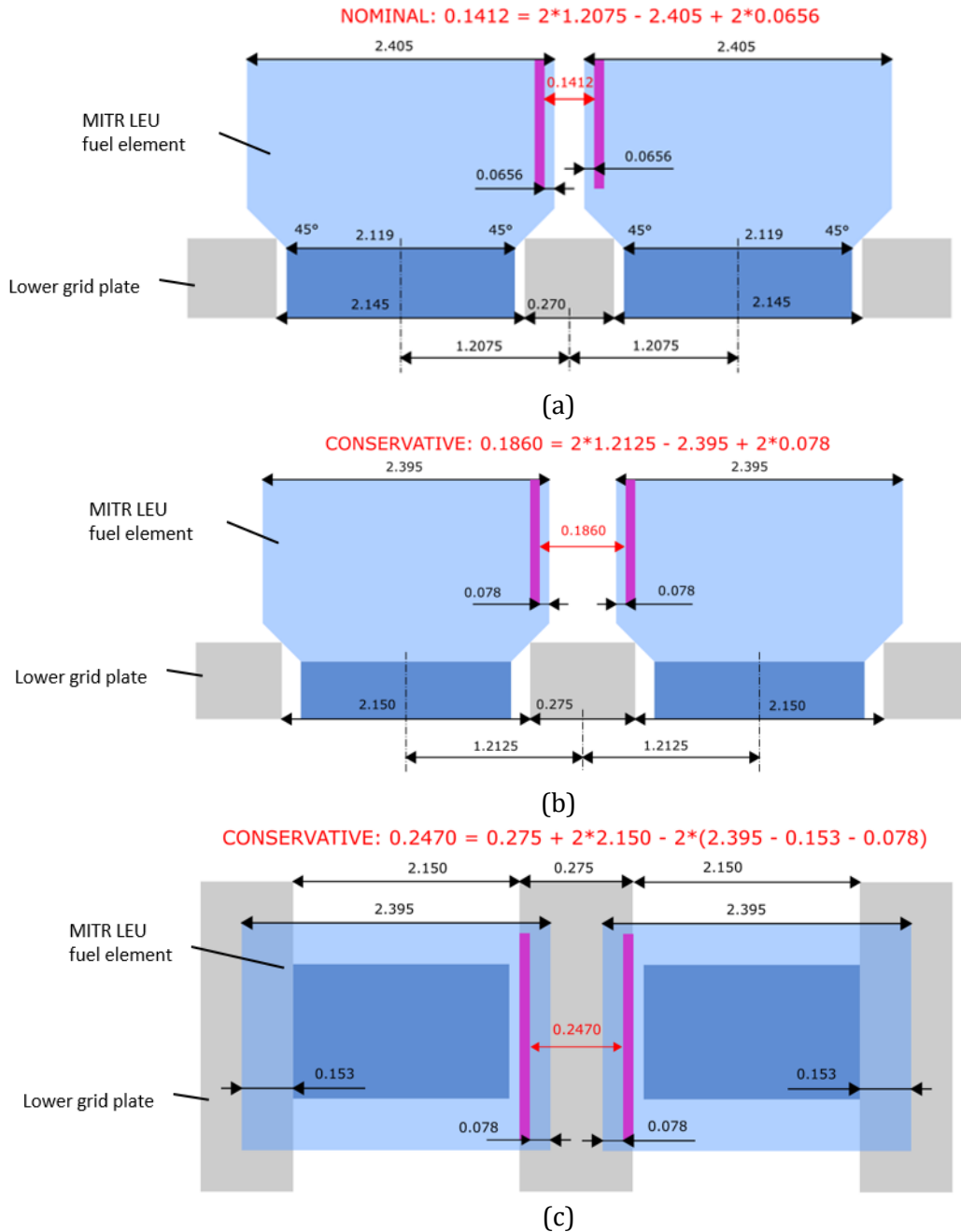


**Figure 3.2. Schematic of calculating combined coolant channel gap thickness: (a) nominal (side view), (b) conservative without lift (side view), (c) conservative with lift (top view). All dimensions in inch. Not drawn to scale.**

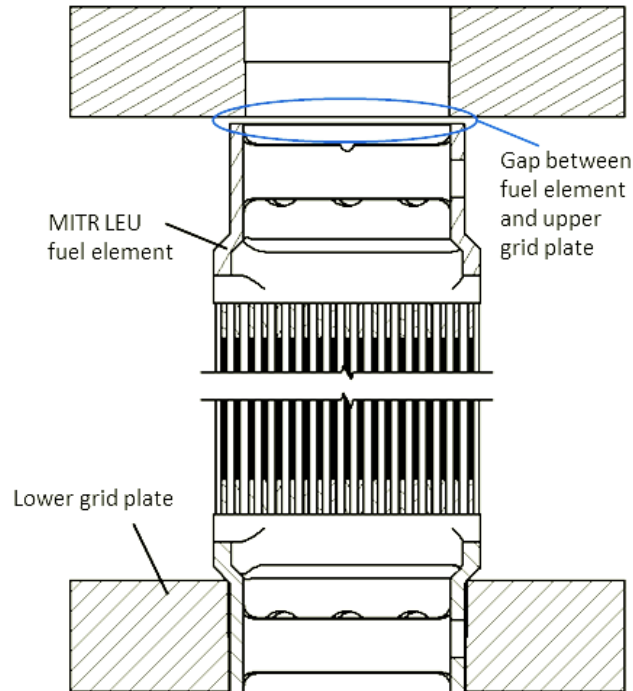


**Figure 3.3. Schematic of the MITR LEU element on the lower grid plate (in scale).**

## 3.2 Summary of Design Parameters

In preparation for the flow test campaign, design parameters for hydraulic testing of the LEU fuel element have been reviewed and documented in [38]. These relate to design needs of the reactor and, are therefore, referred to as reactor design parameters since they do not take into account design margins required for the experimental test design and other purposes. Nominal and other design basis conditions that may lead to more limiting requirements for the LEU fuel element hydraulic performance have been analyzed. In this section, only a summary of this review is presented.

The coolant flow rate per element was estimated on the basis of the flow network analysis, which provides the target test value of the inlet condition for the flow test. To evaluate the flow distribution and the pressure differential on the plate under the given inlet condition, a more detailed CFD analysis, which takes into account the 3D shape of the element, including the end fittings, will be performed during the preliminary stage of the flow test design.

It has been determined that the most limiting flow conditions may occur during the first LEU transition core. According to the proposed LEU transition core plan [39], the MITR will start with 22 fresh LEU fuel elements and gradually change to 24 fuel elements arranged in an equilibrium configuration, while the remaining five or three fuel element positions will be occupied by solid aluminum dummy elements. Given that almost no coolant flows through the dummy elements, the start-up phase of the LEU core is expected to have the highest coolant velocity within the channel gaps of the fuel elements. Therefore, the flow conditions present in the start-up phase of the LEU core with 22 LEU elements will be targeted in the flow test. Given that the MITR transition plan has not yet been finalized, the flow rate per element of the equilibrium core with 24 fuel elements (under normal operating conditions) is also analyzed to provide a range of possible inlet flow rates in the

flow test. The detailed fuel orientation and channel structure of this core setup can be found in references [38] and [40].

The hydraulic reactor design parameters for the MITR LEU are summarized in Table 3.2. One key parameter for the flow test is the channel gap thickness of the combined end channel (two end channels facing each other), which determines the maximum channel size disparity and the maximum hydraulic force (induced by pressure differential) on the fuel plate. The combined end channel gap thickness is 0.141 inch for nominal value and 0.247 inch for maximum conservative value due to dimensional tolerances. For the flow test, although a single fuel element will be tested in HMFTF, the combined end channel dimension will be represented in the flow test through the basket design.

Another key design parameter is the flow rate per element. For the transition core with 22 fuel elements, the flow rate of the target element (with one 0.247-inch-thick outer channel) is 123.4 gpm. For the equilibrium core with 24 fuel elements, the flow rate of the target element (with one 0.247-inch-thick outer channel) is 113.3 gpm, based on a nominal total primary coolant flow rate of 2400 gpm. Note that the value of flow rate per element was increased to account for the additional flow area from the combined end channel gap. Temperature influences target test value selection due to the impact of water density on the pressure differential in the test. However, temperature itself is not necessarily a primary design parameter. Until the capability of HMFTF to match the desired temperature range is clarified, water temperature is listed as regime appropriate. Other design parameters, including system pressure and coolant chemistry, are also listed as regime appropriate, but their influence on the flow test results is less significant.

**Table 3.2. MITR LEU hydraulic reactor design parameters for flow test.**

Design parameters	Specification	Core condition	Hydraulic reactor design parameter	Type
Flow rate	22-element	2400 gpm	123.4 gpm	Primary design parameter
	24-element	2400 gpm	113.3 gpm	
Combined end channel gap <sup>a</sup>	Nominal	0.141 inch	0.247 inch	Primary design parameter
	Conservative within tolerances	0.247 inch		
Temperature	-	44 °C-55 °C	-	Regime appropriate
System Pressure <sup>b</sup>	-	Atmospheric	-	
Chemistry	pH	5.5-7.5	-	
	Conductivity	<5 $\mu$ s/cm	-	
	Chlorides	<6 ppm	-	

<sup>a</sup> See Figure 3.1 for case (b).

<sup>b</sup> The pressure at the top of the upper plenum is atmospheric. The coolant level is 10 feet above the top of the fuel plates [4], therefore at the core outlet, the pressure is 1.31 bar [40].

The review of the hydraulic reactor design parameters for MITR [38] also estimated the uncertainty of flow rate per element and channel velocity distribution. The flow rate per element presented in Table 3.2 was calculated using the primary coolant flow rate of 2400 gpm, the bypass factor of 0.921, and the corresponding channel geometry specification. The flow rate per element can be higher if uncertainties in the primary coolant system measurements and flow distribution within the core are

considered. The primary flow measurement uncertainty is estimated at 5% [4]. The flow distribution uncertainties for MITR LEU cannot be estimated. The uncertainties estimated in the past for the HEU core can be used as an approximate value. The flow distribution measured with Pitot tubes for MITR-II exhibited a maximum flow rate per element of up to 12.1% higher than the average flow rate per element [6]. By multiplying the factor of 105% associated with the primary flow uncertainty by the factor of 112.1% associated with the flow distribution, the maximum flow rate can be calculated as up to 117.7% of the nominal value. In the previous hydro-mechanical stability experiment for the MITR-II HEU fuel, a factor of 120% was used to represent the maximum possible flow rate [6], which provides another reference value for the upper limit of the per-element flow rate.

A summary of the nominal and conservative per element flow rates for both the 22-element core and the 24-element core is provided in Table 3.3. The conservative values are calculated using the two options mentioned above: one is combining the 5% primary flow uncertainty and the 12.1% flow distribution uncertainty; the other is using 20% to represent all uncertainties. The second option with the 20% uncertainty is suggested for the flow test, because of the conservatism and consistency with the previous MITR-II flow test. Therefore, the maximum inlet flow rate for the flow test is 148.1 gpm for the 22-element core and 135.9 gpm for the 24-element core. Flow distribution within one element has been estimated using the flow network approach and is presented in [38].

**Table 3.3. Summary of the nominal and conservative flow rate per element.**

Core	Thick end channel gap thickness (inch)	Flow rate per element (gpm)		
		Nominal value	117.7% of nominal value	120% of nominal value
22-element	0.141	108.1	127.2	129.7
	0.247	<b>123.4</b>	145.2	<b>148.1</b>
24-element	0.141	99.1	116.6	118.9
	0.247	<b>113.3</b>	133.3	<b>135.9</b>

To characterize the type of structural response expected from the fuel plates during the flow test, the coolant velocities in the channels must be estimated. Reference [38] includes a flow network analysis that aims to estimate these velocities. The limitation of this method should be noted since it simplifies the MITR LEU geometry into parallel channels and considers averaged effects. Therefore, the velocities that are indicated as the same (or very close) for the one vs. 24-element cases would be expected to be somewhat different considering the effects of end fittings and some local effects on the flow distribution. Table 3.4 presents a summary of that analysis while the details can be found in [38]. The average velocity is expected to be around 5.00 m/s and 2.77 m/s in the thick outer channels and the inner channels, respectively.

**Table 3.4. Comparison of velocity for one-element model and full-core model.**

Flow network model	Inlet flow rate (gpm)	Internal channel velocity (m/s)	Thick end channel velocity (m/s)
24-element	2400 (7.9% bypass)	2.54	4.61
One-element	113.3 (for 24-element core)	2.54	4.61
22-element	2400 (7.9% bypass)	2.77	5.03
One-element	123.3 (for 22-element core)	2.77	5.01

### 3.3 Expected Behavior of the Plates

The design of the flow test and in particular the design of the testing vehicle, as well as the selection and placement of the sensors used in these tests to achieve the goals defined earlier, are driven by the expected type of behavior of the plates under the hydrodynamic load and the magnitude of that behavior. Deformations of a fuel plate due to its interaction with the flowing coolant can be categorized as steady-state deflections or transient oscillations. Steady-state deflections are primarily induced by a pressure differential between the two sides of the plate. A pressure differential develops when the channel gaps on the two sides of the plate have dissimilar thicknesses, and the coolant flows through them at a different velocity. The differences in the channel thickness usually come from the design specifications, manufacturing tolerances (causing non-uniformities in the shape of the plate or its tilt in the side plate grooves), or a combination of both. Oscillations of the plate may be induced by fluctuations in the coolant flow that originate from the vortex shedding from reactor structure components, fuel element end fittings, or the plate edges exposed to the flow. Sufficiently high flow rates may lead to a plastic collapse of the plates and closure of the channels that may be preceded by gradually increasing permanent (plastic) deflections, non-negligible large oscillations, or a sudden collapse.

#### 3.3.1 Critical Velocity Estimation

To predict the behavior of the plates, the coolant velocities in the channels (estimates presented in the previous section) have been compared to the critical velocity, a threshold velocity originally defined by Miller [9] (see Section 2.1 for background information). If the expected velocity in the coolant channels is well below Miller's critical velocity, the pressure differential is expected to be the primary driver of plate deflections and quasi-static deflections rather than large-scale oscillations of the plates are expected. The following equation has been used for the critical velocity estimation for a flat plate with fixed boundary conditions [9]:

$$V_c = \left[ \frac{15Ea^3h}{\rho b^4(1-\nu^2)} \right]^{1/2} \quad (3.1)$$

where  $V_c$  is the critical velocity beyond which the plate could collapse due to large-scale oscillations,  $E$  is the Young's modulus of the plate,  $a$  is the plate thickness,  $h$  is the channel gap thickness,  $\rho$  is coolant density,  $b$  is the channel width, and  $\nu$  is the Poisson's ratio of the plate. The Miller's velocity for the MITR LEU core was calculated to be 16.65 m/s [3]. In this evaluation, aluminum properties were used for the plate. Note that here the thin channel gap size (0.070 inch) and the plate thickness (0.046 inch) are the minimum within the fabrication tolerances, which makes the calculated Miller velocity more conservative. The Miller's velocity calculated using the nominal thicknesses for plate and channels is 18.90 m/s.

The ratios of the predicted flow velocities from Section 3.2 to Miller's critical velocity have been calculated for the conservative scenario with lift and are listed in Table 3.5. The basic Miller's formula has been developed for channels with an identical thickness on both sides of the plate. In the most conservative case that is analyzed here, there is a large disparity in the channel gap thicknesses (0.070 vs 0.247 inch). The maximum velocities in these two channels are estimated at 2.79 and 4.99 m/s, respectively. It is expected that Miller's formula is less reliable for cases with such large channel gap thickness disparities. Thus, the actual threshold velocity around which oscillations are more

pronounced may be different. Nonetheless, this estimation should provide a first-order check of the nature of the plate's behavior.

**Table 3.5. Miller's critical velocity calculations for MITR LEU plate.**

Channel type	Velocity in channel $v$ (m/s)	Critical velocity $v_c$ (m/s)	Ratio of $v/v_c$
Thin LEU	2.79	16.65	0.168
Thick LEU	4.99	31.28	0.160

If the Miller's velocity is estimated separately for the thin and thick channel gaps and then actual coolant velocities are compared to these values, the ratios are 0.17 and 0.16 for the thin and thick channel gaps, respectively. These computed quantities from the ratios are well below Miller's critical velocity. For this reason, pressure differential induced quasi-static deflections are expected to be the primary mode of the plate's response to the hydrodynamic loading expected during the operation of MITR with LEU fuel, and vibrations of the plate at significant magnitudes are not expected.

### 3.3.2 Expected Magnitude of Plate Deflections

An important aspect of the sensor selection for monitoring the deflections is the magnitude of the expected deflections. While most of the past experiments, especially those studying collapse of the fuel plates, did not require high-resolution measurements, the deflections of the MITR LEU plates operating under the nominal and conservative conditions described in Section 3.2 of this report are expected to be in the range of only a few mil. Recently, a detailed FSI analysis has been performed to estimate the magnitude of the plate deflections in MITR LEU elements [3]. Since the preliminary safety analysis [4] did not include an estimation of the flow-induced deflection, this FSI analysis provided a preliminary assessment of these deflections. The analysis considered ideal and imperfect shapes of the plates, nominal and conservative sizes of the outer channel gaps and both nominal and conservative flow conditions.

Figure 3.4 presents the distribution of the displacements on the plate that was characteristic for all the analyzed cases. The plate deflected the most near the leading edge, at the centerline of the plate. None of the imperfections in the shape or orientation of the plate within the grooves of the side plate, as attempted in [3], had a significant influence on that displacement distribution on the plate.

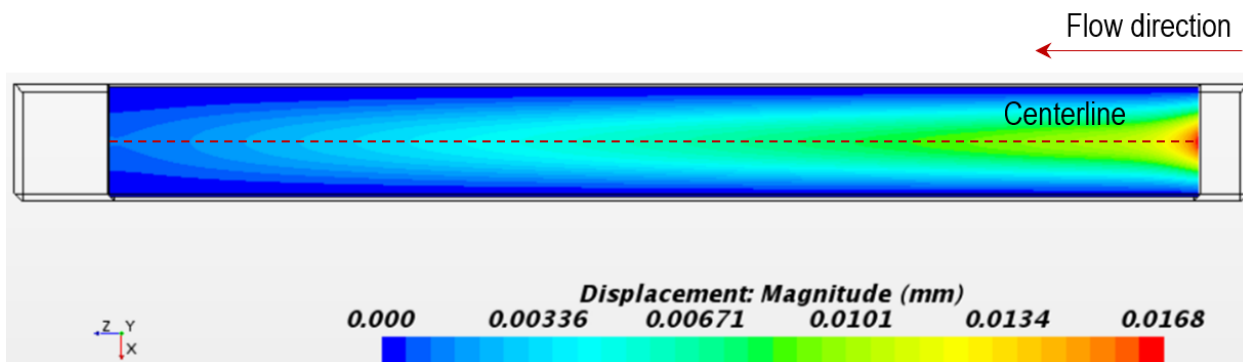


**Figure 3.4. Plate displacement contour for nominal geometry and flow conditions.**

Table 3.6 lists four out of 14 analyzed cases in [3]. The cases listed here highlight the significance of the geometrical tolerances in the MITR LEU fuel element and the MITR core. The nominal size of the

outer channel gap thickness is considered in Case 1. Case 4 considers a possible lift and larger separation of the two neighboring fuel elements whose outer channels face each other in the core. Case 6 additionally considers the tilt of the plate, while Case 7 considers imperfections in the plate following the 10<sup>th</sup> mode of natural vibrations. The magnitude of the imperfections introduced in the geometries of the plate used in cases 6 and 7 was scaled to the maximum allowed fabrication and assembly tolerances.

**Table 3.6. Description of selected cases in the FSI analysis [3].**

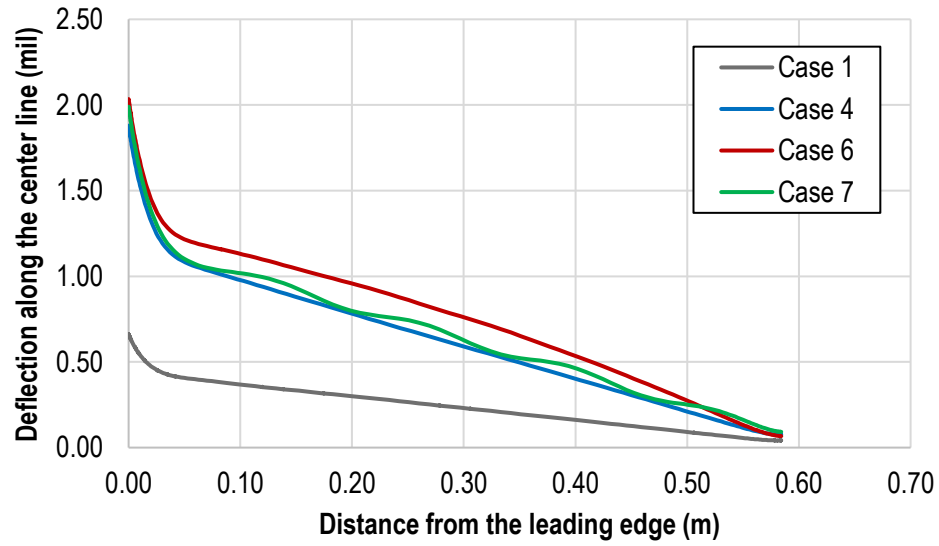
Case #	Thick-channel size (inch)	Thin-channel size (inch)	Plate thickness (inch)	Inlet flow rate (kg/s)	Notes
1	0.141	0.0746	0.049	1.13	Nominal geometry and flow conditions
4	0.247	0.070	0.046	2.13	The most conservative (largest) thickness of the outer channel gap with fuel lift considered, nominal flow conditions
6	0.2425–0.2515	0.070–0.079	0.046	2.13	The plate is slanted within the groove of the side plate, nominal flow conditions
7	0.247	0.070	0.046	2.13	Plate deformed using 10 <sup>th</sup> mode of vibrations, nominal flow conditions

Figure 3.5 presents deflections of the MITR LEU plate due to FSI along the centerline for the four cases described earlier. Note that maximum deflection occurs at the leading edge, then reduces in value by 40% within the first 0.05 m (~2 inch) back from the leading edge, and then linearly reduces to nearly zero at the trailing edge of the plate. The addition of geometrical imperfections to the shape of the plate (tilt and a wavy shape following the 10<sup>th</sup> natural mode) did not significantly change the character of the response of the plate. Past experiments with flat plates that had more pronounced imperfections [25] indicate that at some scale, the imperfections start to dominate the character of the response of a plate to the hydrodynamic load. The magnitude of deflections in the middle of the length of the plate in the axial direction in these experiments was comparable to the magnitude of the deflections at the leading edge. This is not the case shown in [3] for the MITR LEU fuel plates with imperfections no greater than the specified fabrication and assembly tolerances.

This analysis has the following implications for the design of the sensors monitoring the deflection:

1. The sensors should be sensitive enough to capture deflections of magnitude around 2 mil (50 micrometer),
2. The uncertainty of the measurements must be less than the maximum expected magnitude of the deflections, and
3. The sensors should be installed as close to the leading edge of the plate as possible to increase the chance of capturing such small deflections.

It should be noted that the analysis reported in [3], was performed for a single plate with fixed boundary conditions on the long edges and the effect of the flexible side plates was not considered. For that reason, the deflection of the plates in the tested element may be larger, but it is not expected to have a significant impact on the scale of the predicted maximum deflections.



**Figure 3.5. Deflections of the MITR LEU plate due to FSI along the centerline.**

## 4 Initial Design and Conceptual Testing of Sensors

### 4.1 Data Gathered and Its Purpose

The sensors to be used during the flow test at HMFTF can be divided into two groups based on their primary purpose:

1. To monitor the flow conditions in the loop, and
2. To monitor the structural response (deflections and oscillations) of the fuel plates under the hydrodynamic load.

The sensors serving the first purpose are mostly an integral part of the HMFTF loop. These sensors were already tested at the HMFTF and proven to work during other testing campaigns supporting the USHPRR conversion [30], [31], [32], [41]. Their ranges of operation and uncertainties are known and previously reported by OSU [27], and for that reason, they do not require further testing in preparation for this flow test, except that the Pitot tube assembly will require redesign to fit the end fitting of the MITR LEU element.

Most of the sensors serving the second purpose need to be selected and acquired for further preparatory testing as the type of measurements required during this flow test is different from those of the other test campaigns conducted at OSU (characterization of small deflections of plates was not the primary goal of other test campaigns). Since the fuel plates are expected to deflect no more than a few mil, while at the same time access to the measuring locations is obstructed (the leading edge of the outer plate is not accessible because of the presence of the end fitting), the applicability of these newly selected sensors needs to be thoroughly investigated before they are chosen to be used in the actual flow test of the MITR LEU element. The exceptions in that group are those strain sensors that have been extensively tested by OSU staff during the GTPA testing campaign [32], [31].

The applicability of sensors for the below-listed measurements and observations must be demonstrated in the later (preliminary and final) stages of the flow test design, using a single flat plate and an all-aluminum mock-up:

1. Leading-edge visualization,
2. Deflection measurement,
3. Flow rate measurement,
4. Pressure drop measurement, and
5. As-built geometry measurements.

During the operation of the flow loop, the pumps generate heat that the cooling system of the facility must dissipate. The amount of generated heat varies depending on the required flow rates, and pressure drops through the tested specimens. During the GTPA tests, owing to limitations on cavitation within the test loop and around the test specimen at high flow rates, some tests were performed at elevated temperatures of 175 °F and 250 °F [32]. Based on the communication between the Argonne subject matter experts (SME) and the OSU HMFTF SME, the HMFTF operating temperature could have a lower limit as high as 250 °F (120 °C) for the MITR LEU flow test, which is significantly higher than both the MITR inlet and outlet coolant temperatures (44 °C and 55 °C, respectively).

Elevated temperature and pressure may influence the accuracy of some of the measurements or even make some sensors inoperable. Thus, the measurement capabilities, including the uncertainty levels under the flow conditions expected at the OSU HMFTF flow loop, must be well understood before the LEU element testing.

A test with a surrogate system generating a similar pressure drop as the MITR LEU fuel element in the testing basket is required during the preliminary stage. It will allow to better understand the temperature that can be achieved in the loop in the actual tests of the MITR LEU element. Where the temperature of the coolant in the surrogate test, and hence the LEU fuel element flow test remains within the operational range of the coolant in the MITR core, no further evaluation would be required. However, if the temperature during the flow test is higher than coolant temperatures in MITR, then the impact of these parameters on the conclusions of the hydro-mechanical evaluation of the MITR LEU fuel element must be evaluated. Modifications to the OSU HMFTF flow loop may be requested if that impact on the outcome of the test is determined to be substantial.

### **4.1.1 Leading-edge Visualization**

As stated in Section 1.3 of this report, the goal of the flow test is to prove that integrity of the fuel element is maintained, and unacceptable deformations do not occur under the selected testing conditions that envelop the operational conditions of the MITR accounting for uncertainties in the flow conditions. Since, as currently predicted, small deflections of fuel plates in these elements are challenging to measure, both visualization and measurements of the deflections of the plate's leading edge (where the deflections in the MITR LEU fuel element are expected to be the largest) are of interest at the current conceptual design stage of the flow test. Quantification of the total deflections (elastic and plastic) in the test is desired. However, it is not required for the successful completion of the shakedown tests of the MITR LEU elements. Quantification of the plastic (permanent) deflections is required (see Section 4.2.5 for discussion of the measurement of permanent deflections).

Note that various sensors may only be applicable to selected reactor fuel elements due to different geometries of the plates and the end fittings as well as different levels of accessibility of plates of interest. As explained in Section 3.1, the outermost plates of the MITR LEU element are the most limiting from the FSI perspective. As shown in Figure 4.1 (left), a direct view from the top on the leading edge of these plates is obstructed by the design of the end fitting. Only an angled line of sight through the end fitting allows observation of the leading edge of plates #1 and #19.

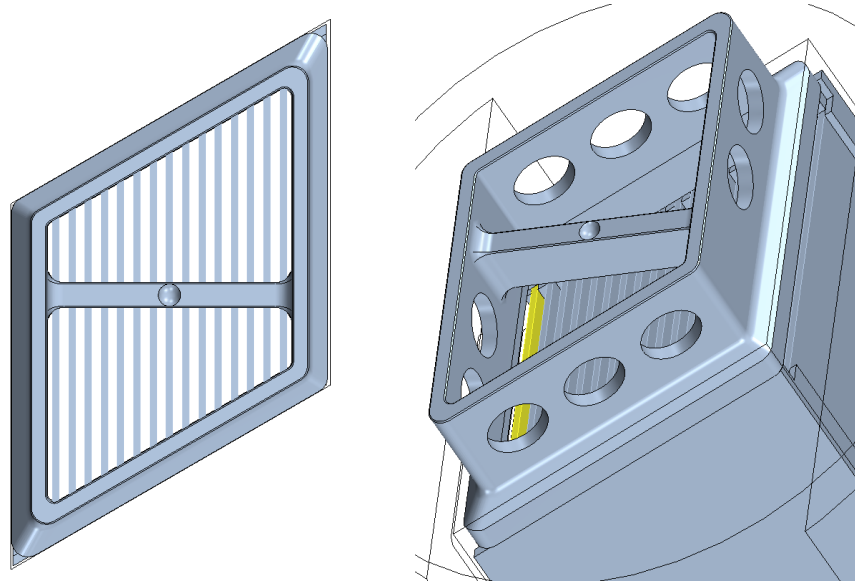


**Figure 4.1. A fully obstructed view of the outermost plates through the end fitting of the MITR LEU fuel element; from the top (left) at an angle (right).**

### 4.1.2 Deflection Measurements

While the position of plates #1 and #19 in the element makes it hard to observe their leading edge from the inlet side of the upward coolant flow a side approach for direct deflection measurement sensors (i.e., for a proximity sensor, laser, etc.) is possible for these two plates. The conceptual design of the test vehicle (basket) proposed in this report takes advantage of this possibility, and a side window or a smaller sensor port is currently included in the design (see Section 5.1 for more details). The final selection of the sensors will guide the design of that port (or window) in terms of its exact location and size.

It is understood that each of the deflection measurement techniques faces its own set of obstacles like interference with the flow, need for external access through the loop piping walls, or difficulty of performing measurements under the selected flow test conditions. These issues are further discussed in sections 4.2 and 4.3 and are planned to be examined comprehensively in the later stages of the flow test design.

### 4.1.3 Total Flow Rate and Individual Channel Flow Velocity Measurement

There is a potential difference between the flow conditions in the core for the most limiting configuration of the two elements whose outer channels face each other and the conditions in the flow test in which only a single element will be tested. During the flow test, a thick outer channel will be formed between the fuel element and the internal walls of the basket. As shown in Figure 4.2, the flow in the outer combined channel gap in the reactor is supplied via the end fittings of the two neighboring elements. The flow between the two elements is not permitted because of the lower grid presence.

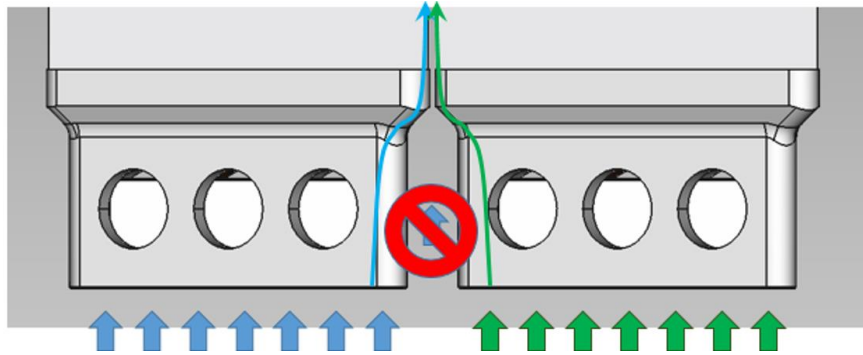


**Figure 4.2. A schematic of the inlet flow in the outer combined channel gap in MITR LEU core.**

Due to the presence of the lower grid, the flow between the elements in the reactor is assumed to be negligible. Since only a single fuel element will be considered in the flow test, the flow into that large outer channel will only be supplied through a single end fitting. Thus, flow disparity in the channels within the element during the flow test is expected to be different from the flow disparity in the reactor. Thus, by adjusting the total flow rate in the HMFTE, the resultant pressure differential on the plate can be matched to that present in the core. These differences are planned to be estimated with the use of CFD during the preliminary stage of the flow test design. During the flow test, the measurements of the total and local flow rates may allow for characterization of the flow disparities and verification of the numerical models.

In addition, significant variations in the channel flow velocity during the test may be an indication of excessive plate vibrations. A sudden drop in the measured channel flow rate may indicate a plate collapse leading to a channel gap closure. The design of the Pitot tube assembly must allow for insertion through the complex shape of the end fittings of the MITR LEU fuel element. The feasibility study must demonstrate that installation of the Pitot tube assembly is possible, and its presence does not significantly alter the flow in the coolant channels and the outcome of the flow test.

#### **4.1.4 Pressure Drop Measurement Across the Entire Element**

Proper measurement of pressure drop across the entire element is required to mimic the in-pile flow conditions. Similar to the flow rate measurements, individual channel pressure drop measurements may be used to better understand the flow disparity factor within the element, and to detect large changes in channel gap thickness during the flow test, potentially due to the collapse of the fuel plates. Pressure taps have been used in the past to monitor pressure drops in each channel of the fuel elements. However, this approach would require drilling multiple holes in the side plates of the MITR LEU fuel element. To meet the goal of this specific flow test, individual channel data is not required. The test is designed so the most limiting conditions occur for the outermost plate. While the individual channel pressure drop was used in the past to identify the loads acting on the plates and detect collapse of the plates, in the current test the deflection monitoring of the limiting plate will be conducted with other techniques. Thus, only the overall pressure drop across the test element is currently of interest.

### 4.1.5 As-built Plate Thickness and Coolant Channel Profile Measurements

The channel gap measurements in the MITR LEU element must be performed for several reasons:

1. The initial as-built shape of the element will be needed as an input to CFD models that will be used for calculations of flow distribution in the element,
2. The outer channel gap is formed by the element and the cut out in the basket together, forming the thick outer channel. The thickness of the outer channel gap will be adjusted by set screws (see Section 5) to match the conservative size established during the review of the reactor parameters (see Section 3).
3. In case the sensors used for monitoring the leading edge during the test provide inconclusive data, the use of a channel gap probe (CGP) between consecutive stages of the flow test may provide information about any permanent flow-induced deformations in the element, which serves the primary goal of the flow test.
4. Monitoring of any failure modes of the entire element is of interest in the flow test. CGP will be used to detect any plastic (permanent) deformations in all plates, not only the limiting one from the FSI point of view.

A feasibility study of available CGPs will be performed before the flow test on an all-aluminum mockup of the MITR LEU fuel element and early versions of the testing basket. The design of the basket must allow for inspecting the outer channel gap thickness and maintaining the relative position of the element within the basket during consecutive test stages (without repositioning of the fuel element).

### 4.1.6 Summary

Table 4.1 contains a list of test items and the purpose of the data to be gathered during the flow test. Three roles have been designated for these quantities of interest: required (R), supporting (S), and optional (O). Focus is placed on visualization (R.1) or measurements of the deflections near the leading edge (R.2) of the plate. Total flow rate measurements (R.3) are required as the total flow rate is a controlling parameter that will be adjusted to meet the required pressure differential across the most limiting (outer) plate. It is understood that the design of the end fittings may make it difficult to use Pitot tubes in the test, so the role of flow rate measurements in each channel (S.2) was designated as supporting. Measurements of the deflections of the plate away from the leading edge are optional.

**Table 4.1. Summary of test items and their purpose in the flow test.**

Role	ID	Test item	Purpose
Required	R.1	Plate leading-edge visualization	The stability of the plates at high flow should be proven by observation (R.1) or measurement (R.2) that would determine the magnitude of elastic deformation if it occurred during the testing. A margin to plastic deformation must be proven by running one or more tests at flows beyond the MITR operating conditions.

Role	ID	Test item	Purpose
	R.2	Plate leading-edge deflection measurement	See the purpose of R.1.
	R.3	Total flow rate	For determination of average flow test velocity
	R.4	Total flow area for the test vehicle	For determination of average flow test velocity
	R.5	Plate thickness for each plate in the as-fabricated element	To support numerical simulation and analyses
	R.6	Dimensional profile of each channel gap	Observe significant fuel element deformations such as plate bending, twisting, or plate detachment from the side plate.
	R.7	Flow area for each channel in the as-fabricated element	To allow simulation
	R.8	Flow area for each of the two end channels	To allow simulation
	R.9	Visual examination of fuel element	Observe significant fuel element deformations such as plate deflection or bending, twisting, or plate detachment from the side plate.
	R.10	Water temperature	Confirmatory data to verify the pressure drop vs. flow relationship
Supporting	S.1	Pressure drop across the fuel element	Confirmatory data to verify the average test flow velocity (R.3 and R.4)
	S.2	Flow rate for each channel	Semi-empirical Moody friction factor treatment could be confirmed; redundant confirmation of average test flow velocity (R.3 and R.4). Pressure taps or Pitot tubes will be used depending on the manufacturability of the setup.
Optional	O.1	Measurement of plate deflections (other locations than the leading-edge)	Although plate leading-edge visualization (R.1) or deflection measurement (R.2) may be sufficient, another method such as a strain or laser measurement could be used at additional locations.

## 4.2 Sensors Previously Used at OSU

### 4.2.1 Sensors Used for Monitoring the Flow

#### 4.2.1.1 Vortex Flow Meters

The primary flow rate measurement instruments used on the HMFTF are Rosemount series 8800D vortex flowmeters. Measurement of pump net flow is provided by dedicated flow meters for each pump branch (FIT-111 for MFP-111 and FIT-211 for MFP-211) and then a flow meter is also installed in the test section (FIT-401) and the bypass leg (FIT-411) as shown in Figure 4.3. This arrangement allows for the verification of instrument operation through the comparison of the measurements (test section flow + bypass flow = net flow) and redundancy in case of an instrument failure by using calculated flow values instead of the direct measurement.

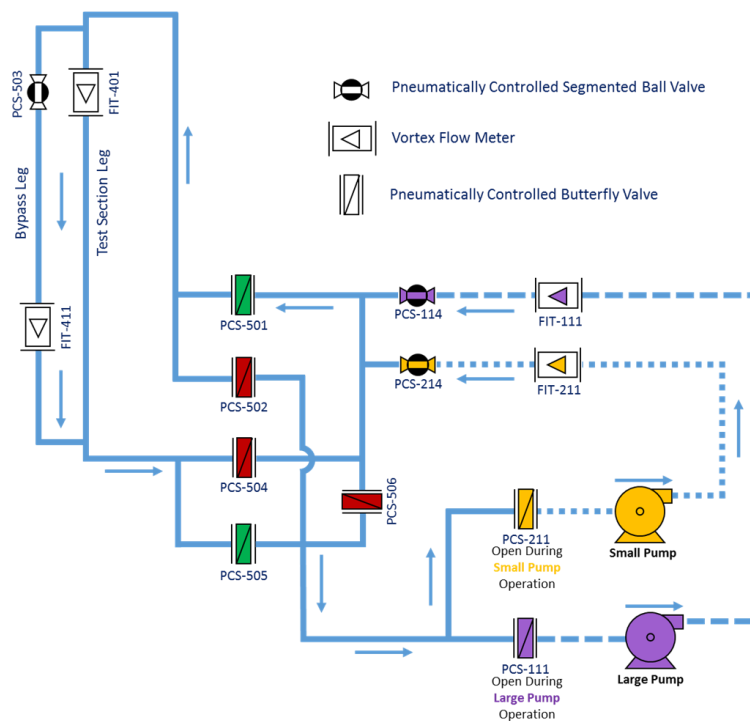


Figure 4.3. Flowmeter Layout.

#### 4.2.1.2 Differential and Static Pressure Instruments

Rosemount 3051 series pressure transmitters are used throughout the HMFTF for both static and differential pressure measurements (with the exception of the Pitot tubes). For quality measurements related to an experiment, both test section inlet and outlet (PIT-501 & PIT-502) static measurements are available as is a dedicated differential pressure instrument (PIT-430) across the test section. Measurement uncertainty for these instruments is presented in [27].

#### 4.2.1.3 Thermocouples

Standard k-type thermocouples are installed throughout the HMFTF to provide required feedback for operators and quality data related to fluid temperatures during a test. In the primary coolant system,

all locations that provide quality data have groupings of 3 thermocouples installed. This arrangement not only provides redundancy and the ability to verify instrument operation but also allows for the reduction in measurement uncertainty through averaging the 3 values at each location. Uncertainty data for this instrument type are presented in [27].

### 4.2.2 Strain Gauges

Exhaustive testing of several types of strain gauges performed at HMFTF has identified that the EK/W series of gauges from Vishay PG is the best performer found to date. A special process has been developed at OSU for installing and verifying these instruments prior to testing [42]. These instruments are paired with a PXIe-4330 data acquisition card and have been most successfully used in a simple quarter bridge configuration. However, this card is capable of both half and full-bridge operation as well.

Due to the harsh conditions within the loop, strain gauges have proven to generally not maintain a stable enough zero signal throughout testing to be useful for quantitative characterization of deflection values. However, their very fast response and the system's ability to sample at high frequencies (up to 5 kHz, in general 2 kHz) allowed their use to explore the dynamic response of individual plates within an element under both steady and transient flow conditions during the GTPA testing campaign [32].

Since the tested element will contain LEU, the strain gauges cannot be embedded in grooves machined in the cladding, unless these were created before the fuel plate was bonded by the HIP process. Thus, the only feasible method of attachment is on the surface of the cladding, as described in [42]. This approach creates locally higher spots on the plates, which, together with the attached wiring, may distort the flow in the leading-edge area of the plate.

The expected small deflections of the plate in the tested MITR LEU fuel element under conservative flow conditions may produce a signal that doesn't allow for quantification of the strains and, indirectly, the deformation. Nonetheless, the strain gauges are still considered to be potentially useful, for reference purposes only, during the evaluation of the other sensors.

### 4.2.3 Fiber Optic Gauges

The HMFTF data acquisition system includes a LUNA ODiSI-B system for fiber optic strain measurement that is capable of sampling at up to 250 Hz, although this sample rate is reduced as the sensor length increases. To date, only 2-meter sensors bonded directly to surrogate fuel test plates have been used in the HMFTF. The LUNA system exhibited a much better zero stability when compared to the strain gauges. However, the relatively low sample rate greatly limited the system's ability to acquire dynamic data during the GTPA testing [32]. Experience has demonstrated that once a plate has begun to vibrate to a certain degree, the LUNA system is unable to acquire useful data and it has thus been useful mostly in looking for residual strain at low flow rates after exposure of the element to increased flows. For the MITR LEU, large oscillations are not expected, and these strain gauges may be useful. Another advantage of the LUNA system is that little disturbance to the flow occurs as a result of the sensors and the lead wires that can be attached to the sensors near the leading edge, where the impact on the maximum deflections of the plate is the smallest.

## 4.2.4 Pitot Tubes

Pitot tube assemblies like those shown in Figure 4.4 have been successfully integrated into almost all HMFTF experimental campaigns to date. These measurements have been used to estimate the flow distribution between subchannels in experiments, and to estimate the pressure drop through an experiment within individual subchannels when paired with the bulk inlet pressure measurement. It should be noted that the inclusion of a Pitot tube plate in a flow test will have an impact on the hydraulics of the experiment and it is, therefore, advisable to run an identical test without the Pitot tube plate to allow characterization of this impact. A bottom-up view of the Pitot tube hardware in an experiment is shown in Figure 4.5 to help illustrate the impact of the Pitot tubes on the flow. This view looks into the instrumentation housing and the outlet of the experiment, with the Pitot tube plate entering from the right and extending up into the test section.

Two separate pressure transducers are used to take measurements within each subchannel and an estimate of the superficial velocity in the subchannel can then be calculated using Bernoulli's equation. The first 14 pressure transducers (capable of measurements in 7 subchannels) are Honeywell model TJE instruments and the remaining 10 instruments are Honeywell model A-205 instruments (capable of measurements in 5 subchannels). These instruments have no internal signal processing hardware and are connected to NI PXIe-4330 Wheatstone bridge input cards. This approach allows high-frequency sampling of these channels (up to 5 kHz, normally 2 kHz) using the burst function in the HMFTF control software. Measurement uncertainty for these instruments is documented in [27].

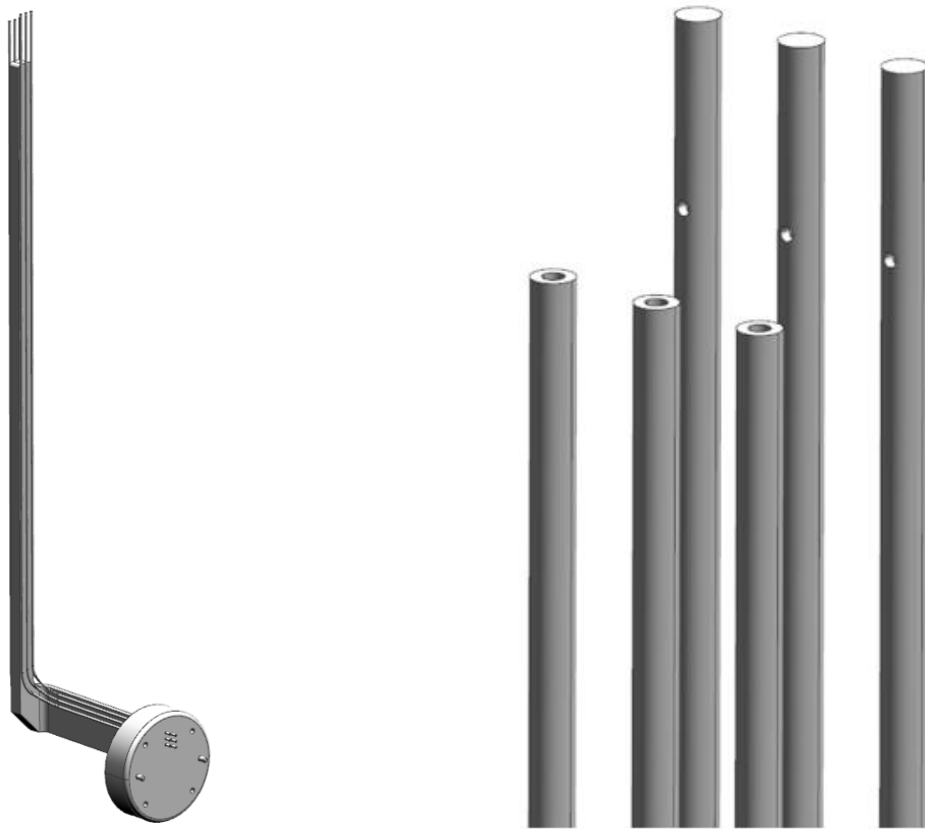


**Figure 4.4. Example Pitot tube plate from AFIP-7 (left) and close up of sensing end of tubes (right).**

There are two obstacles to the use of Pitot tubes for the MITR LEU fuel element flow test:

1. Because of their relatively low rigidity, Pitot tubes require the design of a support structure. A relatively complex path is required to position the Pitot tubes in the outer channels of the MITR LEU fuel element as the tubes would have to go through the narrower end fitting. Thus, the support structure may not reach far enough. If it did, it could potentially block a significant portion of the end fitting opening.
2. The MITR LEU fuel element has 20 channels and accommodating each of them with two tubes is rather unfeasible. The Pitot tubes would have to be designed for a smaller portion of the channel gaps. However, this would unevenly affect the flow in the channels and produce spurious flow disparities in the fuel element.

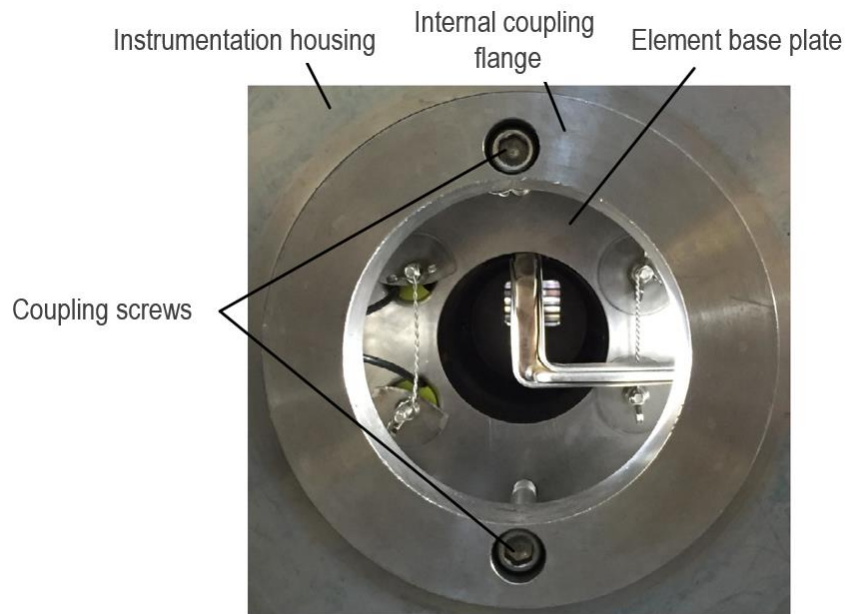


**Figure 4.5. Example of Pitot tube installation in the instrumentation housing.**

#### **4.2.5 Channel Gap Probe**

The CGP is an instrument provided by Idaho National Laboratory (INL) from Capacitec, which allows characterizing subchannel thicknesses in an assembled element (assuming the sabre can access the measurement location). The instrument consists of 2 capacitive probes, one of which faces outward in each direction from the flat sabre, which is 36 inch long. The sabre itself is marked with the distance from the measurement points up the length to the handle down to 1/4 inch.

Data for this instrument is hand-recorded by program personnel as the vendor-supplied software does not allow matching of an insertion distance, or any other notation regarding the position of the instrument, with the recorded channel width data. To maximize the repeatability of this process, dedicated CGP guide blocks have historically been created for each experimental geometry. Guide blocks used have included wire EDM fabricated metal designs as well as 3D printed polymer designs as shown in Figure 4.6. In the past, water droplets within an experiment have also been shown to

impact measurements, and it is therefore important to ensure that the experiment is thoroughly dried before taking measurements with this instrument.

The measurement uncertainty to which this instrument is held to within the HMFTF program is  $\pm 0.0013$  inch [43]. According to the specifications for CGP, it shall be capable of measuring gap thicknesses ranging from 0.050 to 0.240 inch or better. However, the CGP used by HMFTF is capable of measuring channel gaps of up to 0.500 inch. This capability will be sufficient for the target outer channel gap thickness of 0.247 inch in the MITR LEU flow test.

Although access to several external channels of the MITR LEU element is not possible through the end fitting, the design of the basket allows for the measurements of the outer channel gap thickness between different stages of the test. This approach is meant to allow for detecting any permanent deformations in the plate. Even if the position of the element in the basket shifts slightly, a permanent curvature of the plate could still be detected.

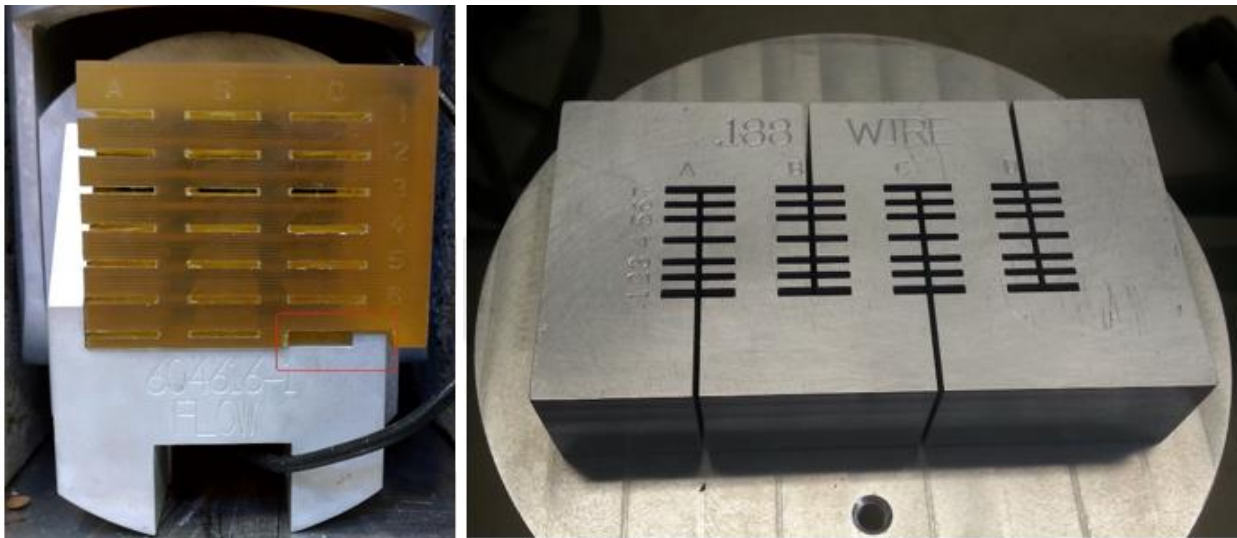


Figure 4.6. Example 3D printed (left) and wire-EDM (right) CGP guide blocks.

#### 4.2.6 Laser Surface Scanner

The laser scanner system at OSU, shown in Figure 4.7, consists of a Gocator 2140 laser profilometer that is mounted onto a gantry stage that is suspended over a granite surface inspection plate. The laser moves along the track to scan the surface of a tested object. The system was successfully used during the GTPA testing campaign to characterize the profile of plastically deformed plates providing significantly higher resolution data than the CGP [31].

The MITR LEU fuel element can be scanned before and after the flow test to determine whether any of the following are observed: permanent deformations in the outer plates, bending or twisting of the entire fuel element, or plate detachment from the side plates.



Figure 4.7. Laser surface scanner at OSU.

## 4.3 Proposed Sensors Requiring Testing

### 4.3.1 Laser Deflection Measurements

Currently, two laser measurement systems have been selected to enable the evaluation of multiple measurement types within this instrument category.

#### 4.3.1.1 1-D Red Laser Spot Measurement

The first laser measurement system is from the Keyence LK-G5000 series of instruments. This system consists of a head that uses a red laser to provide a spot measurement using triangulation of the reflected laser light. A separate controller allows for interaction with the sensor head configuration, setting up automated calculations or alarm set points, and output of data either to a network or to analog outputs.

The specific sensor head selected is the LK-H152 which provides a spot measurement over a diameter of 120  $\mu\text{m}$  and a repeatability of 0.25  $\mu\text{m}$  over a measurement range of 110-190 mm (4.33-7.48 in) as shown in Figure 4.8. The system is capable of sampling at over 10 kHz and should therefore be more than fast enough to meet this project's needs.

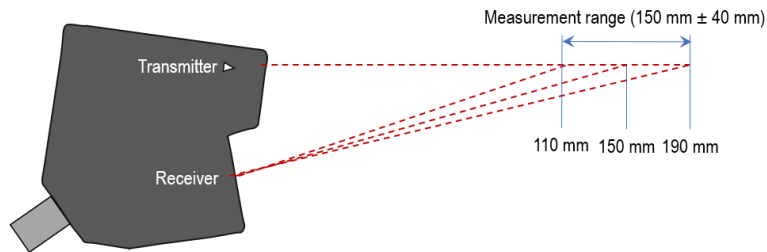


**Figure 4.8. A schematic of Keyence LK-H152 laser measurement range.**

#### 4.3.1.2 2-D Blue Laser Profile Measurement

The second system selected is the Keyence LJ-X8000 series system with the LJ-X8200 sensor head. This system operates in the same way as the LK-G5000 system, but with a blue laser. However, instead of a point reading, it returns many discrete measurements over a line profile. With the dedicated controller OSU has selected, the system is capable of sampling at up to 16 kHz, with measurement ranges and repeatability summarized in Table 4.2 and illustrated in Figure 4.9. The nominal spacing between data points, while in the center of the measurement range, is 25  $\mu\text{m}$  (0.001 inch). Included in this system is the LJ-X800A Raw Data Output Controller which will allow for outputting every sample's full 3200-point profile for storage.

**Table 4.2. Keyence LJ-X8200 measurement specifications.**

<b>Measurement range</b>	Z-axis (height)	245 $\pm$ 34 mm
	X-axis (width)	72 mm $\pm$ 8 mm
<b>Repeatability</b>	Z-axis (height)	1 $\mu\text{m}$
	X-axis (width)	3 $\mu\text{m}$

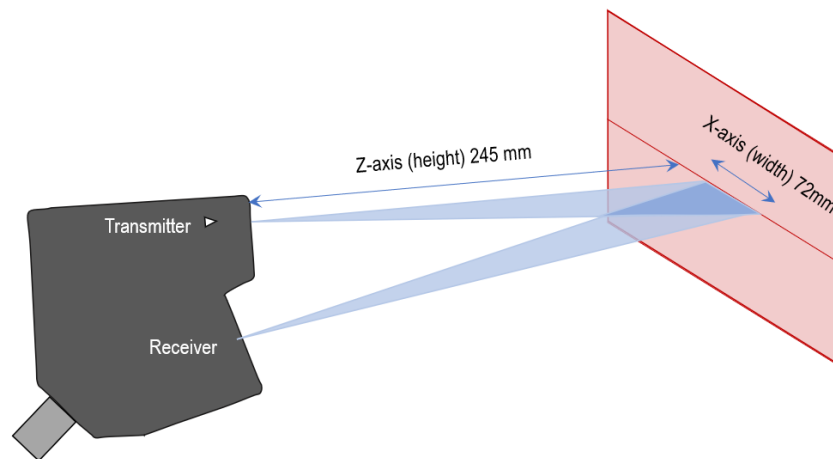


**Figure 4.9. A schematic of Keyence LJ-X8200 laser measurement range.**

Lasers are the least invasive measuring technique for plate deflection as the instrument itself does not protrude into the flow. However, they require a window in the basket, and due to the size of the sensors, will not fit on the basket itself. The outer pipe of the HMFTF flow loop testing section will

most likely need modifications for laser access and attachment. The laser light will have to travel through several media (air, quartz in the window, water in the outer channel gap) to reach the plate and travel back to the sensor. Small vibrations of the element in the basket, the basket itself, or the outer piping may influence the uncertainty of the measurements.

### 4.3.2 Linear Variable Differential Transformers (LVDTs)

Linear Variable Differential Transformers (LVDTs) are a tried-and-true option for measuring displacement and so have been selected here for evaluation. Specifically, the sensor chosen is the model 0234-0000 from Trans-Tek with some customizations to allow for operation at the temperatures and pressures expected within the HMFTF. This model has a 3/8" housing outer diameter, a measurement range of 0.20 inch, and a non-linearity of <0.25% of full scale. Therefore, it should reliably be capable of a 0.0005 inch or better resolution.

Theoretically, due to the construction of this type of instrument, the resolution is infinite and is only limited by the data acquisition electronics used. This sensor will be paired with a PXIe-4340 displacement input module which has a 24-bit resolution and is capable of sampling at over 25 kHz. Accuracy specifications for this module are shown in Table 4.3.

**Table 4.3. PXIe-4340 LVDT sensor accuracy.**

<b>Typical Accuracy ±(% reading + % full scale)</b>	<b>Maximum Accuracy ±(% reading + % full scale)</b>
0.007% + 0.003%	0.025% + 0.015%

Unlike other instruments considered for the plate deflection measurements, an LVDT will need to be integrated into the flow test hardware itself in order to function. The specifications of the currently evaluated LVDT are presented in Table 4.4. These instruments have a smooth outer body and will need to be fixed in place using other hardware such as set screws. A spring-loaded rod (with very small stiffness) can be used to press against the plate and maintain contact with it during the test. The presence of the rod will affect the flow and CFD analysis will need to be performed to assess the magnitude of that effect.

**Table 4.4. LVDT Physical Specifications.**

<b>Specification</b>	<b>Value</b>
Body Diameter [in (mm)]	0.375 (9.525)
Body Length [in (mm)]	0.95 (24.1)
Core Length [in (mm)]	0.55 (14.0)
Core Mass [g]	0.6

### 4.3.3 Inductive Sensor

An inductive eddy current sensor system model eddyNCDT 3070 from Micro-Epsilon has been selected for inclusion in this program. While this is a non-contact measurement technique, it should be noted that the maximum measurement range is 0.4 mm (0.0157 in) with that range starting 0.04 mm (0.00157 in) from the face of the sensor. This means that the sensor head will likely need to be installed partially protruding into the flow channel of any element under test. The influence of that

protrusion on the flow and pressure acting on the plate will need to be determined via CFD analysis as well.

This measurement system has a linearity specification of  $< \pm 1 \text{ } \mu\text{m}$  ( $3.94 \times 10^{-5} \text{ in}$ ), a resolution specification of  $0.1 \text{ } \mu\text{m}$  ( $3.94 \times 10^{-6} \text{ in}$ ), and a sample rate of up to 50 kHz. This instrument should, therefore, be very well suited to characterizing a very slight movement of the plate whether it is a static or dynamic movement.

The sensors selected for further testing under this test plan have an externally threaded body and as such can be installed into a threaded hole in an experiment and then fixed in place with a thread locker and/or jamb nuts. However, it is likely that the instrument received by the program will be customized to some degree to account for greater operating pressures/temperatures and so may differ from that shown.

#### **4.3.4 Contact Sensor**

While contact sensors were proposed as one of the categories worth investigating, a suitable candidate has not yet been identified other than a simple resistance measurement of a closed-circuit probe. The difficulties lie in the conditions of operation expected during the test, which are beyond the range of applicability of the currently investigated contact sensors. Conditions of operations need to be clarified after conceptual design, and therefore if needed, this sensor type could be revisited where there are limitations found in other sensors.

### **4.4 Camera Systems**

After researching options that could be compatible with the conditions within the HMFTF over its operating envelope, only fully externally mounted systems were selected for testing (no borescope type sensors were found applicable). In contrast to the other systems used for measuring the deflections in this flow test, which will observe the plate from a position perpendicular to the plate surface and flow direction, the camera systems will observe the plate from a position looking at the leading edges of the plate(s), along the flow direction. Attempts will be made to quantitatively resolve the magnitude of the plate motion using camera data. However, camera data could also be used to observe qualitative motion and/or vibration or to look for phenomena such as channel collapse.

#### **4.4.1 Machine Vision System**

The first system selected is a Keyence CV-X series machine vision system. This is a fully integrated, industrial machine vision system with a separate camera, controller, and lighting modules to allow extremely versatile configurations. The camera selected is the CA-HF2100M which is a monochrome 21MP camera that is capable of operating at a maximum of just under 50 frames per second. While this speed is not high enough to resolve most expected plate vibrations, the possible benefit of this system is its ability to directly output displacement measurements, whereas a high-speed camera will require post-processing of video files (and storage of those raw video files) to back out displacement data.

The camera will be paired with a CA-LHE50 lens which will allow a pixel resolution of approximately 0.001 inch when positioned with a 4 x 4-inch field of view. Therefore, resolving the desired 0.001 inch of motion will be at the limits of this system as configured. However, it is possible to change the optics on the camera for a smaller field of view as allowed by other test campaigns to achieve a higher resolution.

To provide adequate lighting, this system will include an integrated lighting controller module and a relatively simple light bar assembly. This lighting setup was selected based on the relatively simple geometry and coloring in general encountered at the leading edge of the test plates in experimental hardware tested to date in the HMFTF. If it is deemed necessary, more complicated lighting systems could be integrated in the future which may allow measurement of 3-dimensional features and/or improved measurements with surfaces of varying colors.

#### 4.4.2 High-Speed Camera

As an alternative to the machine vision system, a regular high-speed camera will also be tested. In this case, a Phantom VEO 340L which is already available in the research group from other projects, will be used. When operated at the full resolution of 4 megapixels, the maximum frame rate for this camera model is 800 fps. As the operating resolution is reduced, the maximum frame rate increases as shown in Table 4.5. Note that these are just a selection of common resolutions, and many other options are available with their own corresponding maximum frame rate.

**Table 4.5. Common resolutions and corresponding frame rates.**

<b>Resolution</b>	<b>Frames per Second</b>
2560 x 1600	800
1600 x 1600	1190
2048 x 1080	1460
1280 x 720	3310

This camera system will allow recording of data at a much higher rate than the machine vision system but will be operating at a lower resolution. If one considers a 4 x 4-inch field of view (a general, conservative area to fully cover the inlet of almost any experiment that would be tested in the HMFTF), the system would have a pixel resolution of 0.0025 in (0.0635 mm), and as such would not be able to resolve any plate motion below that value. To back out quantitative plate-deflection values from the data recorded by this system, post-processing of the high-speed video will be required. This procedure will increase the burden on program personnel, owing to the complexity of the experimental setup associated with image processing codes that may need to be unique to each flow element or geometry tested. If high-speed cameras, in general, were selected for full integration into the HMFTF data acquisition system, a likely recommendation would be to procure a dedicated high-speed camera system for HMFTF which could operate at higher resolutions than the VEO 340L, to more finely resolve plate motion.

## 4.5 Conceptual Design Sensor Testing Matrix

During the flow test conceptual design stage, candidate sensors have been selected that have the potential to monitor the deflections of the fuel plates in the MITR LEU fuel element during the flow test. These sensors have been briefly discussed in the previous sections of this report. Currently, a plan for a feasibility study of these sensors is being developed.

The demonstration of the sensors' capabilities should initially be performed on a single flat plate under dry conditions. Subsequently, the sensors that are capable of resolving small deformations should be tested in submersed conditions without flow ("fish tank test"). Sensors that pass this testing stage should be tested in the EFL on a surrogate flat-plate assembly with water flowing through the assembly. Also planned is an all-aluminum mock-up element, to be available in the later stages of the design, together with the basket for further testing in the HMFTF flow loop.

Table 4.6 lists all the types of sensors described in sections 4.2, 4.3, and 4.4. Columns 3 and 4 of the table indicate the sensors for which dry and submersed bench testing demonstration is requested. The need for and practicality of such demonstrations can be reassessed during the preliminary stage. If a specific sensor from groups 1 and 2 (leading-edge visualization and deflection) shows superiority over others during the dry and wet bench tests in terms of sufficient accuracy and projected ease of use within the MITR fuel element test setup, it should be the first one tested in the EFL.

This testing will make use of the following assumptions and steps:

1. Flow test in HMFTF with a surrogate system inducing the same pressure drop as the MITR LEU element at the flow rates planned for the flow test will be performed. This is to determine the temperature and pressure of the coolant during the flow test of the MITR LEU fuel element. (As indicated in Section 4.1, modifications to the OSU HMFTF flow loop may be requested based on this test.)
2. All demonstration testing will use AA6061-T6 and/or -T0 flat plates of similar proportions to GTPA plates 4 inch x 24 inch x 0.050 inch with clamped boundary conditions.
3. Static dry bench testing will be performed, and measured deflections will be compared with those measured with strain gauges and LUNA fibers in two stages:
  - a. Resolve static deflections of 1 mil to confirm the ability to measure small deformations of plates.
  - b. Run a pluck test to characterize the dynamic response of the instruments.
4. Submersed bench testing (fish tank)
  - a. Resolve static deflections of 1 mil.
5. Develop calibration standards and procedures for instruments that have passed steps 3 and 4.
6. Flow test in EFL.
  - a. Develop EFL test section with instrument wiring and optical access to test plate side and leading edge (as applicable to instruments being tested).
  - b. Comparison with deflections measured by strain gauges and/or LUNA fiber is considered

Concurrently, OSU will assemble a new data acquisition system, most likely based on a National Instruments PXIe chassis, to accommodate all the different instrument types. This system will be required to handle this range of instruments at the speed and accuracy that will be required during the flow test. The HMFTF data acquisition system is a PXIe system, so any cards used in this work scope could then be directly applied to the HMFTF flow loop if instruments are chosen for integration.

**Table 4.6. Conceptual Design Sensor Testing Matrix.**

ID	Measurement type	Possible sensor type (Currently assumed model for testing)	Static dry bench testing	Submersed bench testing (no flow required)	Notes
1	Leading-edge visualization	Borescope (no model identified for testing)	X	X	Data acquisition through the end fitting.
		External camera (Keyence CA-H2100M)	X	X	A side window in the basket is required.
		High speed camera (Phantom VEO 340L)	X	X	A side window in the basket is required.
2	Deflection	LVDT (TransTek series 230)	X	X	Perpendicular side feedthrough in the basket is required.
		Laser (Keyence LJ-X8200) (Keyence LK-H152)	X	X	Perpendicular side window required. Possibly mounted outside of the HMFTF flow loop testing section.
		Inductive eddy current proximity sensor (Micro-Epsilon eddyNCDT 3070)	X	X	Perpendicular side feedthrough in the basket is required.
		Strain gauges (EK/W series from Vishay PG)			Unless substantial improvements over GTPA experiment results are expected, further investigation of the strain gauges' use is not required.
		Fiber optic sensor (LUNA)			Unless substantial improvements over GTPA experiment results are expected, further investigation of the fiber optic sensor use is not required.

ID	Measurement type	Possible sensor type (Currently assumed model for testing)	Static dry bench testing	Submersed bench testing (no flow required)	Notes
		Contact sensor (no model identified for testing)	X	X	Perpendicular side feedthrough required. May be used with or without adjustable distances between runs.
		Ultrasonic proximity sensor (no model identified for testing)	X	X	Perpendicular side feedthrough required.
3	Flow	Vortex flow meter			No demonstration needed.
		Pitot tube assembly for channel flow	X		Fitting testing on a dry all-aluminum mockup in the basket is required.  Testing in the HMFTF flow loop is also required once the basket and an all-aluminum mockup are available.
4	Pressure	Static pressure transmitters			No demonstration needed.
		Differential pressure transmitters			No demonstration needed.
5	Pre- and post-test geometry	Capacitive channel gap probe (Capacitec based CGP)			No demonstration needed.

ID	Measurement type	Possible sensor type (Currently assumed model for testing)	Static dry bench testing	Submersed bench testing (no flow required)	Notes
		Micrometer (no model identified for testing)	X		Flow channel spacing before and after flow test.
		Laser surface scanner (Gocator 2140 laser profilometer)			No demonstration needed; Calibration required.
6	Vibration	(not currently planned, see Section 3.3)			Although not currently planned, HMFTF has the capability for installing accelerometers on the basket to monitor the vibrations of the system.
7	Temperature	Thermocouples			No demonstration needed.

## 5 Test Vehicle Design

### 5.1 Test Vehicle Design Requirements

To meet the goal of the flow test planned at the HMFTF at OSU, the following broad requirements have been identified for the flow test basket:

- R.1. The outer dimensions of the basket must allow for insertion to the testing section of the HMFTF flow loop,
- R.2. The internal dimensions of the basket should represent the most limiting configuration in the MITR LEU core,
- R.3. The geometrical features of the basket must be machinable with the techniques and equipment available (EDM cutting, max 20-inch segments),
- R.4. The basket must allow for the installation of the sensors as selected by OSU and Argonne and inspection of the element between stages of testing,
- R.5. The basket needs to be structurally sound enough to not deform during handling, assembly, and the flow test.

A set of design constraints based on these requirements have been defined and are listed in Table 5.1.

**Table 5.1. Design constraints for the flow test basket for the MITR LEU fuel element.**

Constraint ID	Requirement ID	Design constraint
C.1	R.1	The nominal internal diameter of the OSU flow test section is 6.065 inch, the tolerances (cylindricity) of the pipe manufacturing [44], [45] and tolerances of the basket assembly need to be taken into account in the design so the basket fits inside the flow loop without interference.
C.2	R.1	The basket is planned to be connected by screws going through a coupling flange to the instrumentation housing. The end caps of the basket must have mating grooves for the instrumentation housing of the HMFTF loop [46].
C.3	R.2	Gaps between the basket caps and the end fittings of the fuel element must be large enough to avoid any contact between these components during the flow test.
C.4	R.2	To recreate the size of the combined outer channel (as described in Section 3.1), a part of the channel must be machined out of the inner wall of the basket. The thickness of that outer channel gap is targeted at 0.247 inch during the test.
C.5	R.2	The basket design must allow for fine-tuning of the outer channel gap thickness by controlling the position of the element.

Constraint ID	Requirement ID	Design constraint
C.6	R.2	The outer channel gap thickness on the opposite side has a flat surface – no machining is required. The outer channel gap thickness on that side is targeted at 0.054 to 0.078 inch based on the nominal thickness and fabrication and assembly tolerances.
C.7	R.2	The current size of all the gaps around the element within the basket is 0.020 inch unless requested otherwise (the combined thick channel is an exception here); Shells must be cut in such a way that the element cannot be squeezed in the basket.
C.8	R.2	The internal spacing of the channels is controlled only within the plated region of the fuel element.
C.9	R.3	The basket must be machined from AA6061.
C.10	R.3	Each section of the basket cannot be longer than 20 inch due to EDM equipment limitations.
C.11	R.3	Shells for the basket are modular and each can be made from a single 6-inch diameter billet if this allows for tighter tolerances.
C.12	R.3	To avoid sharp corners for the EDM cutting, the cross-section of the basket should be built of two halves cut along the longer diagonal of the MITR LEU fuel element cross-section.
C.13	R.4	Basket end caps should be made of a single solid piece to facilitate its removal.
C.14	R.4	The end fittings of the MITR LEU fuel element should be entirely covered by the basket caps, so the tolerances of fuel element assembly (end fitting to side plate welding) do not affect the position of the element in the main portion (shells) of the basket.
C.15	R.4	MITR is designed with an upward flow of the coolant. Thus, the window/sensor port must be located on the bottom of the basket (near the leading edge of the fuel plates), and the instrumentation housing must be located on the top of the basket (near the trailing edge of the fuel plates).
C.16	R.4	One shell (only) has a window near the leading edge. The shape and the size will be determined in accordance with the investigation done at OSU.
C.17	R.4	Another replaceable shell is needed that, instead of a window, has just a ½ inch diameter hole as a placeholder for other types of sensors (contact sensor, LVDT, inductive proximity sensor, etc.).

Constraint ID	Requirement ID	Design constraint
C.18	R.4	A cutout for wires should be made, running from the window or the hole for the sensor parallel to the flow (axial direction) towards the instrumentation housing. The diameter of the cutout (currently about 3/8 in.) is a placeholder and will change depending on the number of wires. The cutout may be removed from the design at later stages if the selected sensors are installed through the walls of the HMFTF loop testing section.
C.19	R.4	The MITR LEU element needs to be constrained in such a way that the large channel gap maintains constant thickness (~0.247 inch) during the test through a combination of spring-loaded set screws and regular set screws. Each constrained motion must have a spring-loaded set screw on at least one side of the constraint so that the thermal expansion of the fuel element does not cause large local forces on the element.
C.20	R.4	At least two cross-sections in the axial direction need to be constrained in the basket. The ability to constrain more needs to be introduced to allow for force distribution across multiple contact points.
C.21	R.4	Orientation of the basket and the fuel element within it must facilitate the installation of the Pitot tubes.
C.22	R.5	The minimum thickness of the walls in the basket should be sufficient to prevent distortions during handling, assembly, and testing.
C.23	R.5	Due to different coefficients of thermal expansion, the rod tying the basket sections together should be made of aluminum as well, possibly with a spring added to maintain the tension.

## 5.2 Conceptual Design of the Test Vehicle (Basket)

As presented in Figure 5.1, the basket has the shape of a cylinder. It is built of six major parts: four shells covering the plated region of the MITR LEU fuel element and two end caps covering the end fittings of the elements. The end caps are designed as identical and are interchangeable.

Figure 5.1 presents an isometric view of the basket with a porthole for displacement monitoring sensors. Since the sensors to be used during the flow test to monitor the leading-edge deflections have not been yet tested at OSU, it is expected that the shape and size of the window or the sensor port may change. Due to their shape and size, these sensors may need to be installed outside of the testing section. In that case, the groove for the internal wiring may not be needed. However, special couplers between the basket and the testing section may be needed for wire management and positioning of the basket in the flow loop. Figure 5.2 presents an alternative design of the basket with one shell having a special window for laser access. If the lasers are proven to work under the expected flow conditions, such a window design will be further incorporated in the preliminary design of the basket. Due to possible harsh conditions during the test, a window built of quartz is desired.

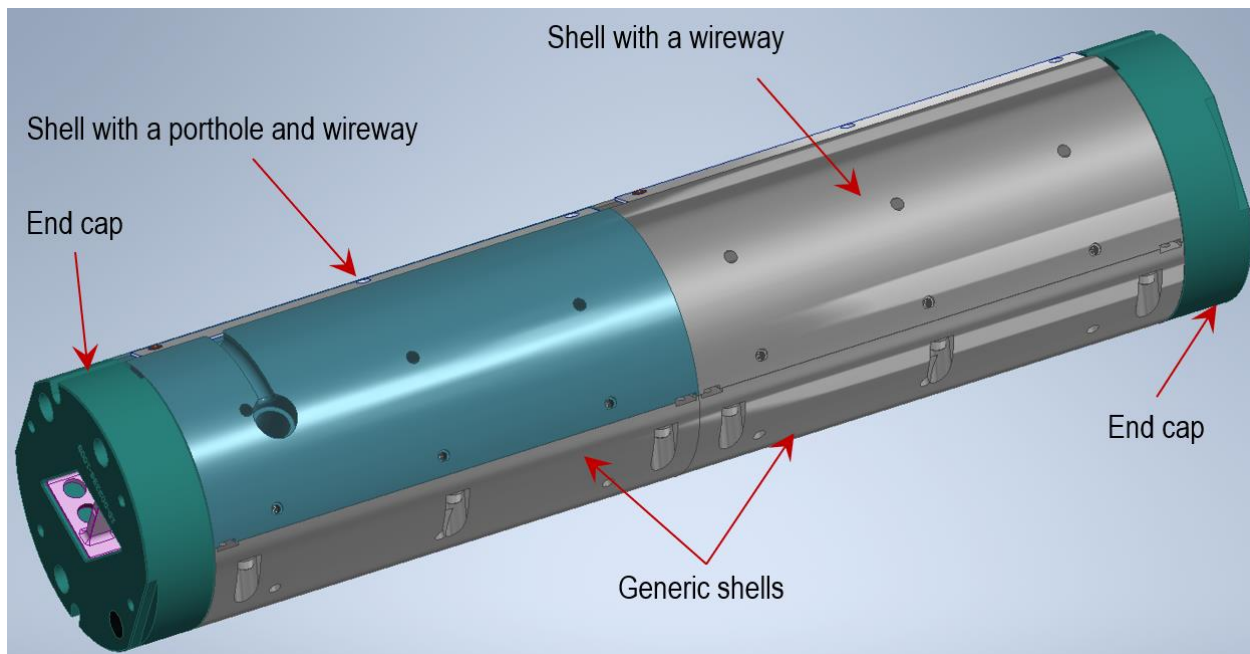


**Figure 5.1. Isometric view of the basket with a porthole for displacement monitoring sensors.**

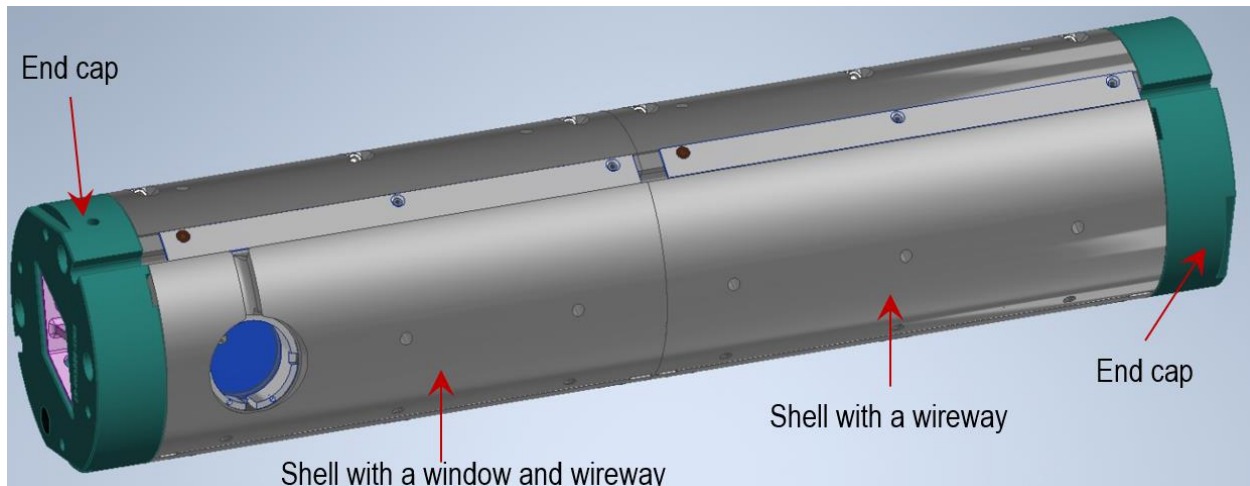


**Figure 5.2. Isometric view of the basket with a window for laser sensors.**

The machining of all basket shells starts from the basic shell shape presented in Figure 5.3. The length of each shell is 11.625 inch, which is within the 20-inch limit of the available EDM machine.

Each shell requires a different amount of machining. There are currently four different types of shells:

1. Two base shells used on the side of the regular outer channel,
2. One shell with wire management groove (which may be removed from the design if sensors are accessing the plate from the outside) and machined outer channel (see Figure 5.4),
3. One shell with wire management groove machined outer channel and sensor port (see Figure 5.5 ), and
4. One shell with wire management groove machined outer channel and laser window (see Figure 5.6). Shells of type 3 and 4 are machined out of the type 2 shell.

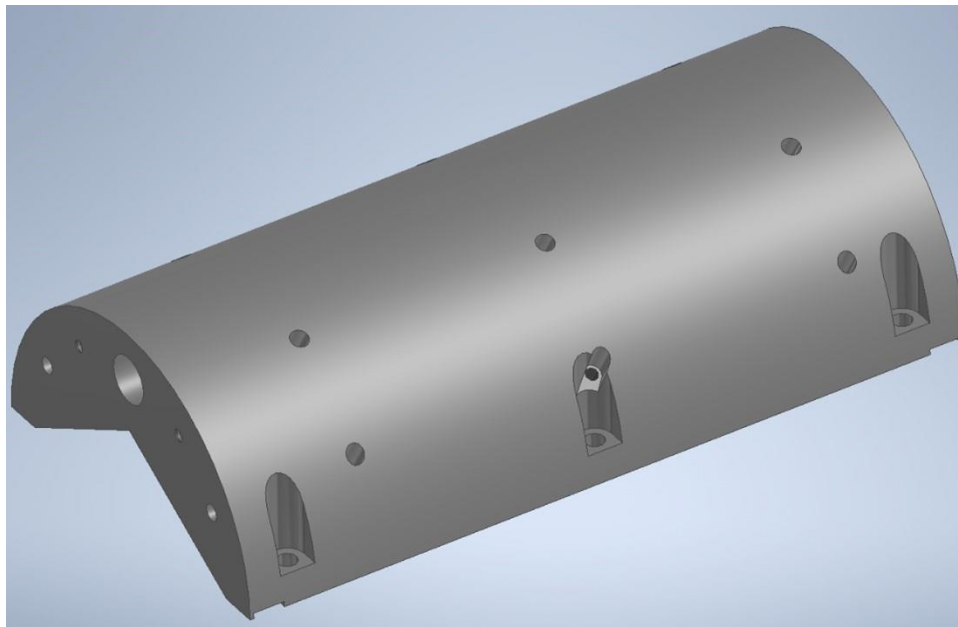


**Figure 5.3. Isometric view of the basket main shell.**

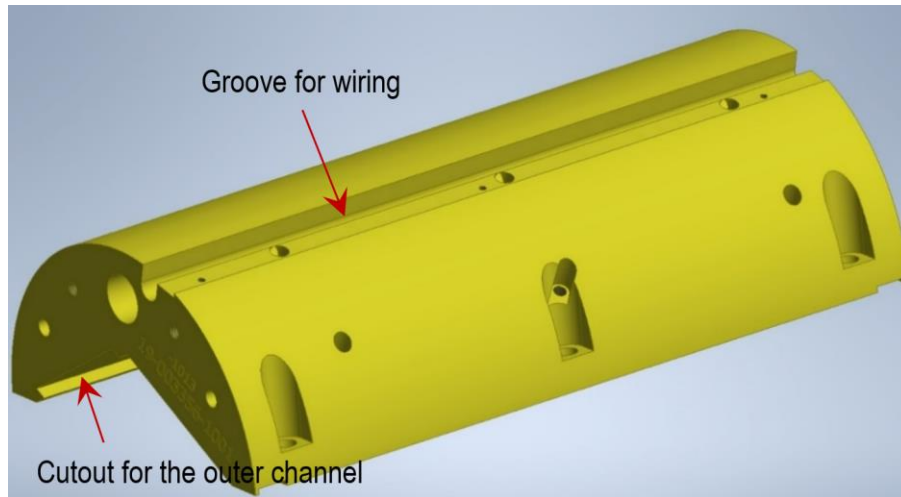


**Figure 5.4. Isometric view of the basket main shell and a groove for wiring.**

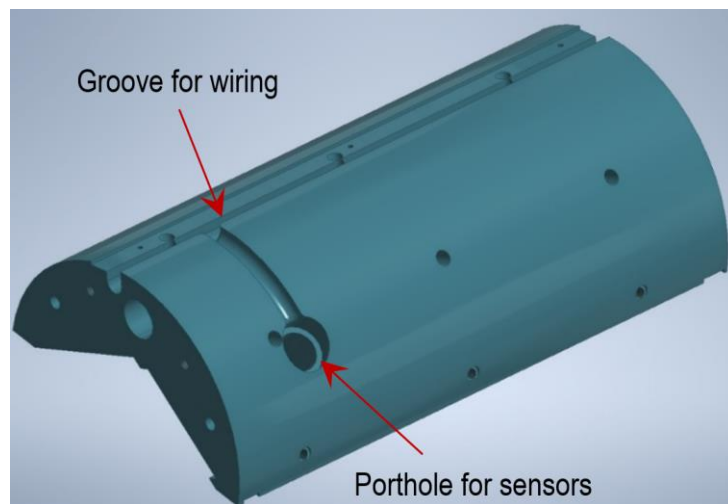


**Figure 5.5. Isometric view of the basket shell with a porthole for displacement monitoring sensors.**

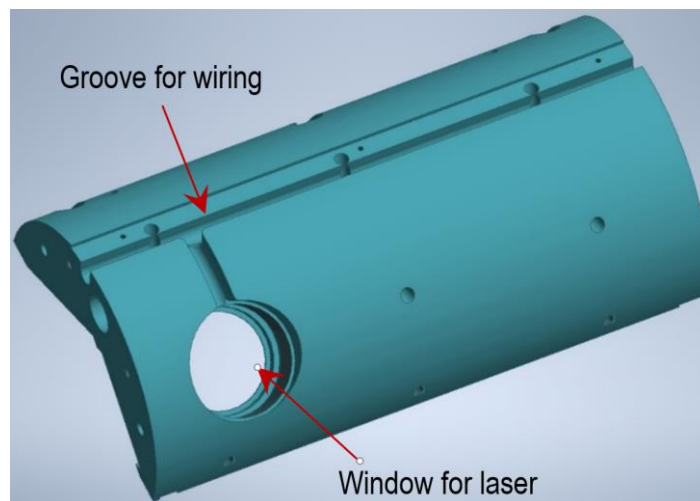


**Figure 5.6. Isometric view of the basket shell with a window for laser sensors.**

Figure 5.7 presents a close-up view of the basket end cap. Grooves are machined out from its outer edge to allow for mating with the instrumentation housing of the HMFTF (see Figure 5.8 for reference). The basket will also be bolted to the instrumentation housing by screws passing through a coupling flange, the instrumentation housing, and into the basket end cap. The exact location of these screws will be established once the orientation of the basket with respect to the Pitot tube assembly is decided upon during the preliminary design stage.

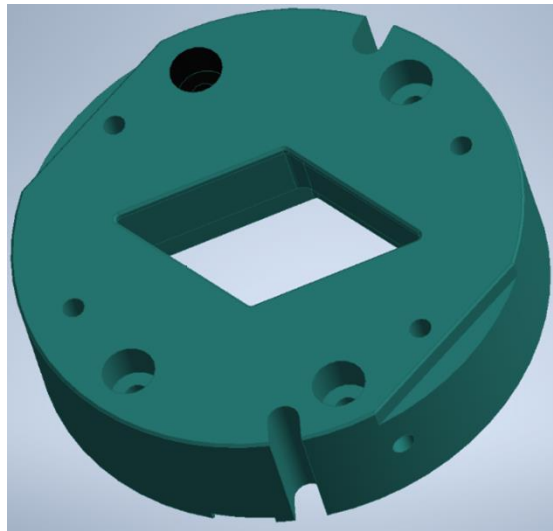


**Figure 5.7. Isometric view of the basket end cap.**

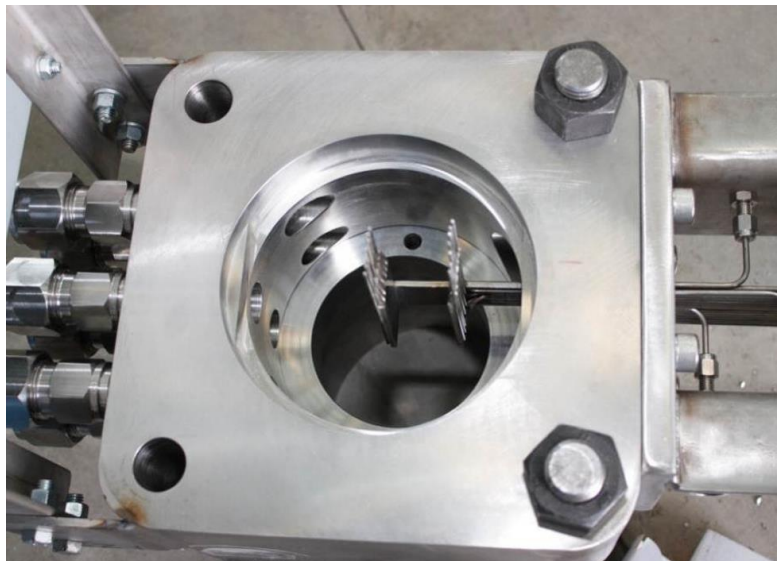


**Figure 5.8. Installation of the basket in the instrumentation housing of the HMFTF.**

The end caps are designed with a lip that reduces possible flow around the fuel element in the flow test. The lip also limits the axial motion of the element within the basket. A silicon gasket is also

considered around the end fitting of the basket to further reduce the axial motion of the fuel element in the basket and reduce the flow. A cross-section view through the basket and the cap is presented in Figure 5.9.

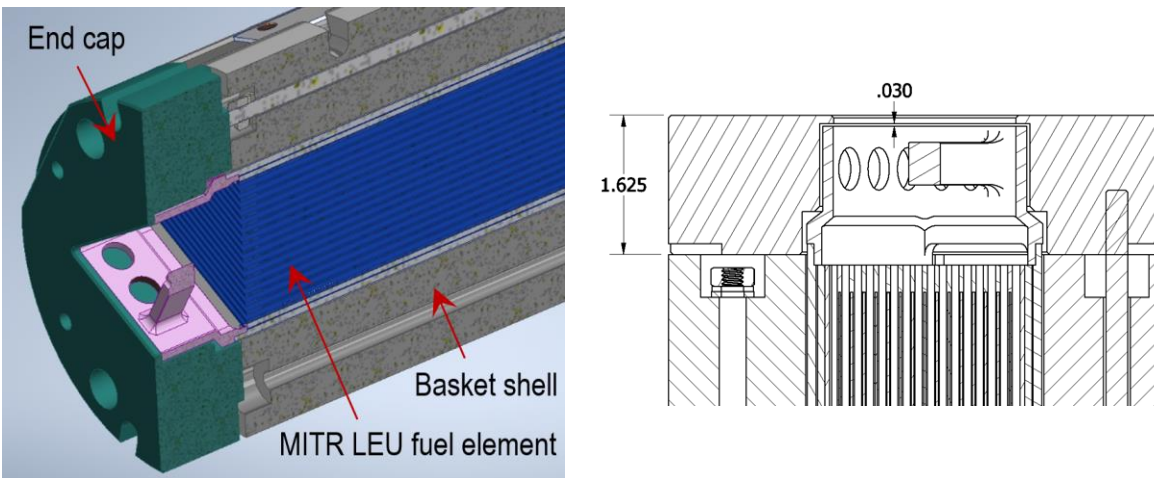


**Figure 5.9. Cross-section through a MITR LEU element installed in the testing basket.**

In the axial direction, the end caps reach beyond the weld line between the fuel element end fitting and the side plate (see Figure 5.10 for reference). This configuration is meant to remove any influence of the fuel element assembly and tolerances around the end fitting on the thickness of the end channels gaps and overall lateral position of the fuel element in the basket. In addition, it facilitates access to the outer channel gap for inspections between various stages of the flow test. If for some reason, reversible (elastic) deformations cannot be traced during the experiment, the irreversible (plastic) deformations should still be observable by CGP without the need for removal of the entire fuel element from the basket in between different stages of the flow test.

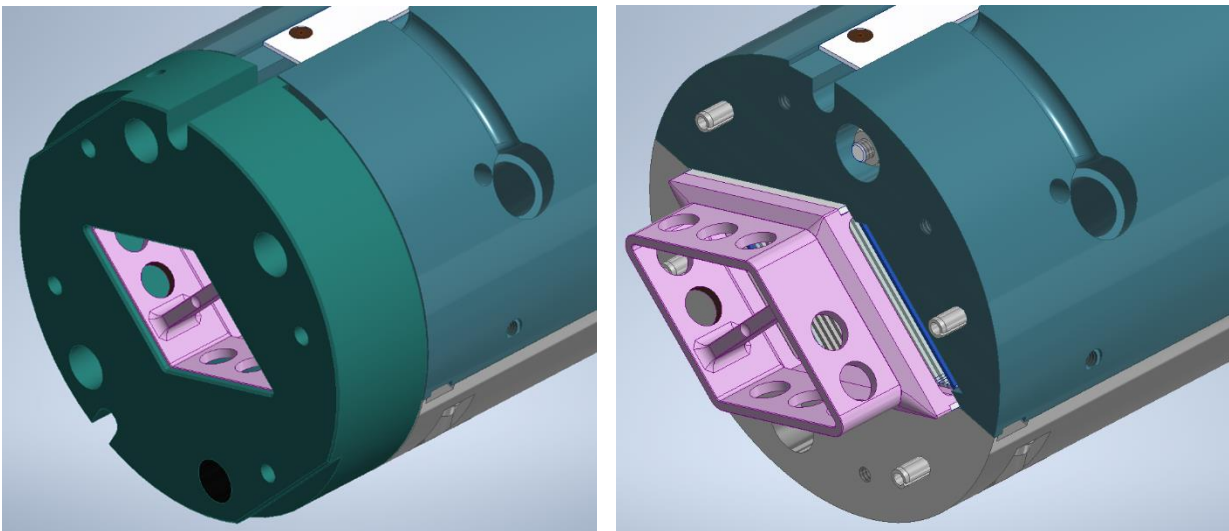


**Figure 5.10. Isometric view of a MITR LEU element installed in the testing basket with (left) and without (right) the end cap.**

### 5.3 Element Constraints in the Test Vehicle

Although a detailed experiment execution plan will be introduced during the preliminary design stage of the flow test, the main stages in the tests have already been considered in the conceptual design as they have an impact on the basket design.

Based on prior experience at HMFTF [41] [31], [32], the presence of the instrumentation required to meet the goal of this experiment in the channel gaps may influence the flow distribution, introduce vortex shedding locations and, as a result, alter the deflection of the plates. Currently, CFD analyses are planned that may help clarify to what extent the selected sensors influence the results when they are present in the flow. Lasers are the least invasive since they can be installed outside of the coolant channels and can access the surface of the plate via a window in the wall of the basket. On the other hand, the presence of the Pitot tubes, LVDTs, or strain gauges may significantly disturb the flow in the channels influencing the outcome of the test.

The MITR HEU fuel element is not fully constrained in the reactor, meaning the element can move laterally and in axially within the confinement defined by the lower and upper grids, reactor core structure, and neighboring fuel elements. The MITR LEU fuel element will have an identical set of constraints to the HEU element. The thickness of the outer channel gap changes due to the changes in the relative position of the two fuel elements forming it. While the flow test aims at replicating the prototypic flow conditions, the only sensors that can measure the deflections of an unconstrained fuel element that are decoupled from the motions of the entire fuel element (including plates' deflections) in the basket are strain sensors. The other methods of monitoring the deflections mentioned in Section 4.3 require that the sensors be attached to the body of the basket with a port for their wiring to exit the HMFTF test section (LVDT, proximity sensor, contact sensor) or a window (laser) only. If the fuel element is allowed to move within the basket, the measurement registered by an external sensor (other than strain gauges) will be comprised of motion of the element and deflection of the plate, and the decomposition of these two will not be possible.

For the reasons mentioned above, the basket has been designed to constrain the fuel element by multiple set screws. These additional, removable (and optional) constraints on the fuel element are designed to allow for simulating various conditions in the basket, but most importantly, to control the thickness of the outer channel gap. Spring-loaded set screws acting directly on the side plates were chosen as the preferred method of constraining the element in the basket as they would allow for fine-tuning of the size of the outer channel gap. Figure 5.11 presents a view of the basket in which locations for the set screws are indicated.

Although the screws only need to be present in two locations in the axial direction to constrain the lateral movement of the fuel element in the basket, there are currently three proposed axial positions for the set screws in each shell of the basket (six total). These multiple locations would limit the forces exerted locally by the set screws on the side plates. The number of axial locations in which the screws need to hold the element will be determined during the preliminary stage of the flow test design.

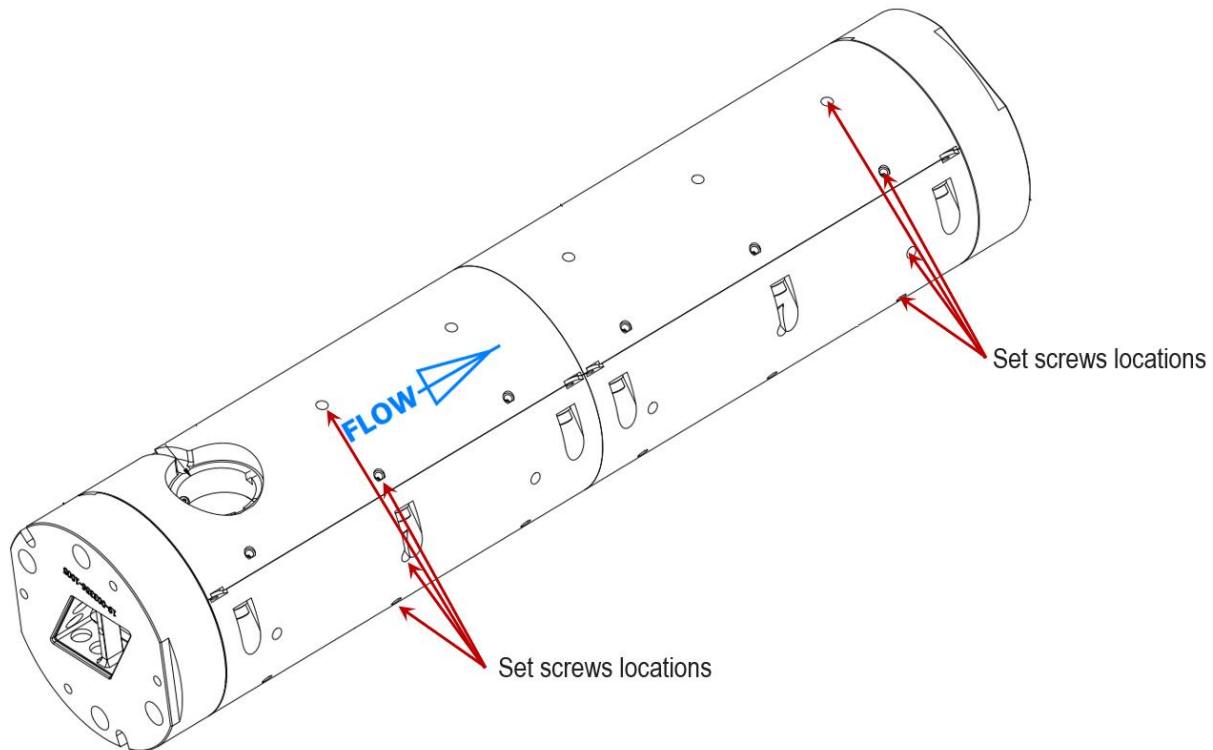


**Figure 5.11. Isometric view of the testing vehicle with potential locations of set screws for fuel element positioning.**

Figure 5.12 shows a representative cross-section with the set screws for positioning of the element. All screws are acting on the side plates of the fuel element only (no point of contact with fuel plates). Due to the limitations on the minimum length of the spring-loaded set screws (red arrows in the figure), some locations can only be secured with regular set screws (blue arrows in the figure). However, along each line of constraints, there is at least one spring-loaded set screw to limit the forces exerted locally on the side plates.

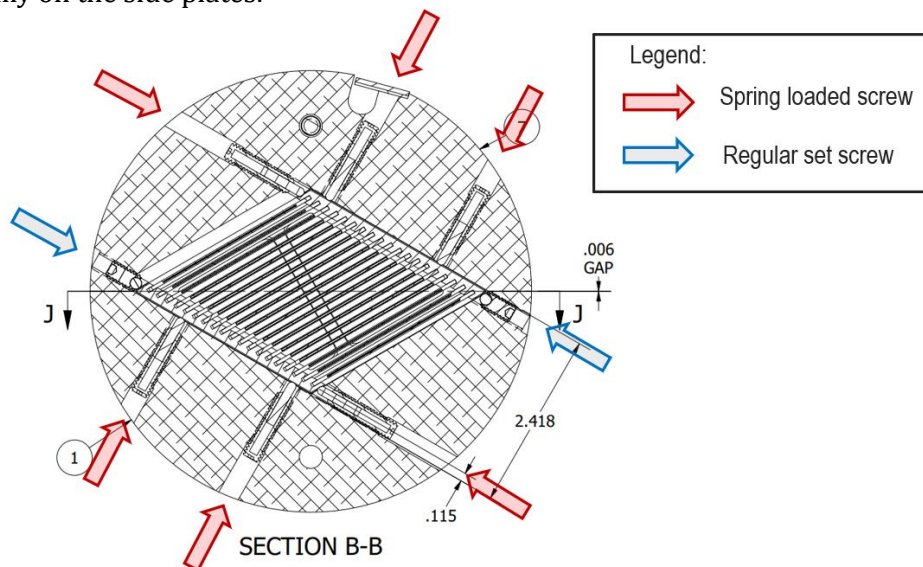


**Figure 5.12. Cross-section view of a MITR LEU element installed in the testing basket with the lateral constraints.**

It is recognized that the preparation of the element for testing within the basket may be difficult with multiple screws requiring adjustment. This method of constraining the fuel element will be tested once the first basket is manufactured towards the end of the preliminary design stage and a surrogate all-aluminum dummy element is available for basket fitting and sensor testing purposes.

The following general stages of the flow test are currently planned:

1. Constrained and instrumented element
  - a. Nominal flow rate, and
  - b. conservative flow rate;
2. Constrained element, without instruments affecting the flow
  - a. Nominal flow rate, and
  - b. conservative flow rate;
3. Unconstrained element, without instruments affecting the flow
  - a. Nominal flow rate, and
  - b. conservative flow rate.

The first stage with a fully constrained fuel element is meant to allow for measurements of pressure-induced plate deflections decoupled from the motion of the element within the basket. The second stage is aiming at testing the element without the influence of the instrumentation in the flow channels. During that stage, transient measurements of deflections will not be possible unless strain gauges directly attached to the surface of the outer plate are used. However, between stages, the CGP measurements could be performed to detect any permanent deformations. The third stage with an unconstrained fuel element aims to test the behavior of the MITR LEU fuel element in conditions as close to the prototypic conditions as possible.

Nominal and conservative flow rates will be used in each stage to investigate the presence of margins to structural failures of the fuel element. The duration of each stage will be determined in cooperation with OSU during the later stages of the design process.

## 6 Activities in Preparation for the Preliminary Flow Test Design

### 6.1 Planned CFD and Structural Analyses of the Element in the Basket

During the work on the conceptual design of the test vehicle and review of the sensors that could be potentially used in the flow test, a need to perform several simulations has been identified. Flow distribution within the tested element may be different from the flow distribution in the fuel elements in the reactor, even though the overall flow rate into the element during the test will match the total element flow rate in the reactor. This possibility is due to the flow differences through the thick outer channel (see Section 4.1 for explanation). CFD analyses are planned to investigate the potential differences in these conditions and establish an equivalent total flow rate for the testing vehicle that will guarantee the same pressure differential is acting on the limiting plate as the one expected in the core.

Almost all the sensors that can directly or indirectly measure the deflections of the plates, as well as the Pitot tubes, will cause flow disturbances within the coolant channels. The exceptions are the lasers or cameras if they can access the leading edge of the plates via a window embedded in the testing vehicle. The influence of the other potentially used sensors (LVDT, proximity sensor, strain gauges with wiring, Pitot tubes, etc.) on the flow, and more importantly, on the deflection of the plates, will be studied in a series of CFD and FSI simulations. Pitot tubes and their supports are expected to partially block the flow in the channels where they will be installed. It is rather impractical to install the Pitot tubes in all coolant channel gaps. This would require 40 tubes reaching the channel gaps through the end fitting. Thus, it is more likely that only a subset of the channels will have Pitot tubes in them. For that reason, the Pitot tubes may unevenly affect the flow in the channels. Sensors like LVDT or proximity sensors will need to partially block the outer channel gap. They also may cause local flow disturbances affecting the pressure acting on the plate surface. CFD simulations may help determine to what extent these effects are relevant for the goal of the flow test. During the flow test, the temperature of circulating water will rise because of the heat generated by the pumps. Not all the heat can be rejected by the cooling system of the HMFTF flow loop. As indicated in Section 4.1, operating temperature could have a lower limit as high as 250 °F (120 °C) for the MITR LEU flow test. The flow rates needed for testing of MITR LEU elements will be lower than those previously needed for other tests [32]. For that reason, such high temperatures may not be observed during the MITR LEU flow test. Nonetheless, thermal expansion analysis of the basket and the MITR LEU element is planned to estimate the dimensional changes of these two components. The analysis aims to assess whether the currently designed gaps between the basket and the element are sufficient to accommodate the assembly tolerances and uneven expansion rate of the tested components. The uneven expansion rate of the tested plates and the vehicle in the GTPA tests have shown to have significant effects in some cases [31], [32]. To allow for a similar magnitude of expansion of the basket and the fuel element, the fasteners for the basket assembly could potentially be made of aluminum as well. Stainless steel fasteners would expand roughly half as much as aluminum due to the differences in the coefficient of thermal expansion.

## 6.2 Basket Fabrication for Fitting Purposes

As mentioned in Section 5, it is understood that positioning the fuel element in the basket may be difficult using the currently proposed method based on an array of set screws. The soft constraints provided by the spring-loaded set screws and regular set screws with plastic ball tips allow for an uneven expansion rate of the basket and the fuel element inside it. To test this method of constraining the fuel element in the basket, the plan is to machine the first version of the basket during the preliminary design stage of the flow test. A surrogate fuel element, in the form of a rhomboid block with the outer dimensions of the MITR LEU element, will also be machined during the preliminary stage. That way, the constraining method can be tested well ahead of the actual flow test. Additional adjustments to the design could be a potential outcome of this fitting test.

## 6.3 Dummy Element Purchasing and Testing

While the sensor testing will be performed during the preliminary stage on a single flat plate, the demonstration of the sensor's ability to measure small deformations on an all-aluminum dummy element installed in the basket must be performed ahead of the actual flow test. The challenges of using some of the sensors are unique to the testing setup required for the MITR LEU fuel element flow test. Thus, to understand the possible difficulties in the use of these sensors and reduce uncertainties in the measurements, purchasing an all-aluminum mockup of the MITR LEU fuel element is currently planned. Dry and submersed testing of the sensors on the all-aluminum mockup is planned to be performed during the preliminary or final stage of the flow test design (subject to availability).

## 7 Summary

In the preparation for licensing, a hydraulic performance evaluation of the MITR LEU fuel element will be performed. Its purpose is to test a prototypic commercially fabricated LEU fuel element, to determine whether any failure modes are observed in the fuel element, including significant deformations such as plate bending, twisting, or plate detachment from the side plate under selected safety basis limits for reactor flow conditions. The evaluation will be performed by a combination of out-of-pile flow test and supporting analyses.

This report describes the activities completed during the conceptual design stage of the MITR LEU fuel element flow test. Three goals have been identified for the conceptual design stage:

1. Review the hydraulic reactor design parameters and identify the most limiting conditions for the fuel plates,
2. Review and select the methods and sensors for monitoring various hydraulic and mechanical characteristics of the flow test, and
3. Develop a conceptual design of the basket to be used in the flow test.

The design parameters for hydraulic testing of the LEU fuel element were reviewed and documented in a separate report [38]. These relate to design needs of the reactor and, are therefore, referred to as reactor design parameters since they do not take into account design margins required for the experimental test design and other purposes. Here, only a summary of that review, containing the information affecting the design of the flow test, is included. The most limiting plate from the perspective of flow-induced deflections in the MITR LEU fuel element is the outermost plate #1 or #19. The most limiting flow conditions in the MITR core occur for two fuel elements whose outer channels face each other. One key dimension in that configuration for the designed flow test is the combined end channel gap thickness, which directly affects the maximum hydraulic pressure differential acting on the fuel plates. Both the nominal and the conservative dimensions of the combined channel are determined on the basis of a review of the technical drawings of the MITR fuel element. The combined end channel gap thickness is 0.141 inch (nominal value) and 0.247 inch (conservative value) because of tolerances. The second important design parameter is the flow rate per element, which has been increased to account for the additional flow area from the combined end channel gap. After this adjustment, the value of the core flow rate per element with 22-element core was estimated at 123.4 gpm, and the value of the core flow rate per element with 24-element core was estimated at 113.3 gpm. The remaining normal operating conditions of the proposed MITR LEU core, including the coolant temperature, system pressure, and coolant chemistry specification, are also summarized (see Section 3 for details).

Together with the design parameters, the expected behavior of the most limiting plates in the MITR LEU fuel element has been described based on the prior experimental work and recently performed preliminary FSI analysis for the MITR LEU fuel element. Because of the low value of the ratio between the calculated coolant bulk velocity in the channel gaps and the Miller's critical velocity for the limiting geometry, pressure-induced quasi-static deflection is the expected type of response of the MITR LEU fuel plates to the hydrodynamic load of the flowing coolant (oscillations of negligible magnitude are expected). The maximum deflections that are expected to occur at the leading edge of the plate are predicted to be in the range of 50 micrometer (~2 mil). This behavior has a direct impact on the selection of the sensors for monitoring the MITR LEU fuel element behavior during the flow test.

Based on the historical experiments, prior experimental work under USHPRR Project, and the needs of the currently designed flow test, sensors for monitoring element behavior, and in particular plate deflections have been reviewed. Most of the past experiments made use of strain gauges installed on the surface of the plate to measure the deflections indirectly from strains. This technique was proven to work for the detection of static deflections as well as dynamic flutter. However, these experiments were mostly focused on characterizing the response of the plates to significant coolant flow rates reaching or exceeding Miller's critical velocity. The flow tests for the USHPRR LEU fuel elements will be executed at significantly lower flow rates that are a fraction of Miller's critical velocity, and hence the expected maximum deflections are small ( $\sim 2$  mil). Sensors that are potentially able to resolve such small deflections are planned to be tested under dry and wet conditions to demonstrate their capabilities before the flow test of the MITR LEU fuel element that will be conducted at OSU. Among them are lasers, inductive sensors, LVDTs, and camera systems. Other types of sensors, like contact sensors, can also be tested if a good candidate is identified. The demonstration tests are planned for the preliminary stage of the flow test design (see Sections 2 and 4 for details).

A conceptual design of the testing vehicle (basket) has been performed under this activity and is also described in this report. Since the flow test will be performed at the HMFTF at OSU, the outer dimensions of the basket allow for insertion into the testing section of the HMFTF flow loop. The internal dimensions of the basket represent the most limiting configuration in the core with the end channel gap thickness equivalent to the conservative thickness of the combined end channel gap. The dimensions of the components building the basket take into account not only the assembly process but also different stages of the planned test, as well as the limitations of the cutting techniques available (EDM cutting, with segments no longer than 20 inch). Since the final selection of the sensors monitoring the deflections will be performed during the preliminary stage, two alternative designs of interchangeable portions of the basket have been proposed. One contains a window that may accommodate laser sensors, and another contains a porthole that may be adjusted in size to accommodate other types of sensors like LVDTs or an inductive proximity sensor. The design of the basket envisions constraining the element to prevent lateral and axial motion of the tested LEU fuel element for a portion of the test so that the displacements of the plate due to the hydrodynamic load can be decoupled from the motion of the fuel element within the basket. The removable end cap of the basket allows for inspection of the fuel element and provides access to the outer channel gap with a CGP between different stages of the test (see Section 5 for details).

Lastly, activities in preparation for the preliminary stage of the flow test design have also been briefly discussed. Section 4.5 describes the planned testing of sensors that have the potential to be used during the flow test of the MITR LEU element for monitoring the plate deflections. Static dry testing and wet bench testing, as well as flow test in the EFL, are envisioned to demonstrate the relevant capabilities of the selected sensors. A series of numerical simulations is planned to analyze in detail the flow distribution within the tested MITR LEU fuel element in the basket. Also, the impact of selected sensors on the flow distribution and the plate deflection is planned to be analyzed numerically. The current plan is that the first basket will be machined during the preliminary stage of the flow test design so an all-aluminum dummy element fitting (subject to availability), and sensor testing, can be performed in advance of the flow test (see Section 6 for details).

## References

- [1] E. H. Wilson, T. H. Newton Jr, A. Bergeron, N. Horelik and J. G. Stevens, "Comparison and Validation of HEU and LEU Modeling Results to HEU Experimental Benchmark Data for the Massachusetts Institute of Technology MITR Reactor," ANL/RERTR/TM-10-41, Argonne National Laboratory, Lemont, IL, USA, December 2010.
- [2] A. Bergeron, E. H. Wilson, F. E. Yesilurt, F. E. Dunn, J. G. Stevens, L. Hu and T. H. Newton Jr, "Low Enriched Uranium Core Design for the Massachusetts Institute of Technology Reactor (MITR) with Un-finned 12 mil-thick Clad UMo Monolithic Fuel," ANL/GTRI/TM-13/15, Argonne National Laboratory, Lemont, IL, USA, November 2013.
- [3] G. Wang, C. Bojanowski, A. Dave, D. Jaluvka, E. Wilson and L. Hu, "MITR Low-Enriched Uranium Conversion Fluid-Structure Interaction Preliminary Design Verification," ANL/RTR/TM-21/2, Argonne National Laboratory, Lemont, IL, USA, July 2021.
- [4] K. Sun, L. Hu, E. H. Wilson, A. Bergeron and T. A. Heltemes, "Low Enriched Uranium (LEU) Conversion Preliminary Safety Analysis Report for the MIT Research Reactor (MITR)," MIT-NRL-18-01 Revision 2, Massachusetts Institute of Technology, Cambridge, MA, USA, October 2018.
- [5] F. E. Dunn, A. P. Olson, E. H. Wilson, K. Sun, L. Hu and T. H. Newton Jr, "Preliminary Accident Analyses for Conversion of the MIT Reactor from Highly-Enriched to Low-Enriched Uranium," ANL/GTRI/TM-13/5, Argonne National Laboratory, Lemont, IL, USA, July 2013.
- [6] G. Allen, Jr, L. Clark, Jr, J. Gosnell and D. Lanning, "The reactor engineering of the MITR-II construction and startup," MITNE-186, Massachusetts Institute of Technology, Cambridge, MA, USA, June 1976.
- [7] M. Hammond, C. A. Lavender, E. Wilson and K. Dunn, "U.S. High Performance Research Reactor Project Functions and Requirements," USHPRR-FR-201 Revision 4, Office of Conversion, Material Management and Minimization Program, National Nuclear Security Administration, U.S. Department of Energy, March 2021.
- [8] W. K. Stromquist and O. Sisman, "High Flux Reactor Fuel Assemblies - Vibration and Water Flow," ORNL-50, ORNL, May 1948.
- [9] D. R. Miller, "Critical Flow Velocities for Collapse of Reactor Parallel-Plate Fuel Assemblies," KAPL-1954, General Electric, Schenectady, NY, USA, August 1958.
- [10] E. B. Johansson, "Hydraulic Instability of Reactor Parallel-Plate Fuel Assemblies," KAPL-M-EJ-9, General Electric Company, Schenectady, NY, USA, July 1959.
- [11] G. S. Rosenberg and C. K. Youngdahl, "A Simplified Dynamic Model for the Vibration Frequencies and Critical Coolant Flow Velocities for Reactor Parallel Plate Fuel Assemblies," *Nuclear Science and Engineering*, vol. 13, pp. 91-102, 1962.
- [12] R. J. Scavuzzo, "Hydraulic Instability of Flat Parallel-Plate Assemblies," *Nuclear Science and Engineering*, vol. 21, pp. 463-472, 1965.
- [13] W. L. Zabriskie, "An Experimental Evaluation of the Effect of Length-to-Width Ratio on the Critical Flow Velocity of Single Plate Assemblies," 59GL209, General Engineering Laboratory, Schenectady, NY, USA, September 1959.
- [14] R. D. Groninger and J. J. Kane, "Flow Induced Deflections of Parallel Flat Plates," *Nuclear Science and Engineering*, vol. 16, pp. 218-226, 1963.
- [15] J. J. Kane, "The Effect of Inlet Spacing Deviations on the Flow Induced Deflections of Flat Plates," *Nuclear Science and Engineering*, vol. 15, pp. 305-308, 1963.

- [16] G. E. Smissaert, "Static and Dynamic Hydroelastic Instabilities in MTR-Type Fuel Elements: Part I. Introduction and Experimental Investigation," *Nuclear Engineering and Design*, vol. 7, no. 6, pp. 535-546, 1968.
- [17] W. F. Swinson, R. L. Battiste, C. R. Luttrell and G. T. Yahr, "Fuel Plate Stability Experiments and Analysis for the Advanced Neutron Source," *Symposium on Flow-Induced Vibration and Noise*, vol. 224, pp. 133-143, 1992.
- [18] W. F. Swinson, R. L. Battiste, C. R. Luttrell and G. T. Yahr, "Structural Response of Reactor Fuel Plates to Coolant Flow," CONF-930702--5, Oak Ridge National Laboratory, Oak Ridge, TN, USA, February 1993.
- [19] W. F. Swinson, R. L. Battiste, L. R. Luttrell and G. T. Yahr, "An Experimental Investigation of the Structural Response of Reactor Fuel Plates," *Journal of Experimental Mechanics*, vol. 9, pp. 212-215, 1995.
- [20] W. F. Swinson, R. L. Battiste, R. C. Luttrell and G. T. Yahr, "Fuel Plate Stability Experiments and Analysis for the Advanced Neutron Source," ORNL/TM-12353, Oak Ridge National Laboratory, Oak Ridge, TN, USA, May 1993.
- [21] M. Ho, G. Hong and A. Mack, "Experimental Investigation of Flow-Induced Vibration in Parallel Plate Reactor Fuel Assembly," in *15th Australasian Fluid Mechanics Conference*, Sydney, Australia, December 2004.
- [22] L. Liu, D. Lu, P. Zhang and F. Niu, "Large-amplitude and narrow-band vibration phenomenon of a foursquare fix-supported flexible plate in a rigid narrow channel," *Nuclear Engineering and Design*, vol. 241, no. 8, pp. 2874-2880, 2011.
- [23] Y. Li, D. Lu, P. Zhang and L. Liu, "Experimental investigation on fluid-structure interaction phenomenon caused by the flow through double-plate structure in a narrow-channel," *Nuclear Engineering and Design*, vol. 248, pp. 66-71, 2012.
- [24] A. J. Castro, N. L. Scuro and D. A. Andrade, "Experimental Investigation of Critical Velocity in a Parallel Plate Research Reactor Fuel Assembly," in *2017 International Nuclear Atlantic Conference - INAC 2017*, Belo Horizonte, Brazil, October 2017.
- [25] A. Tentner, C. Bojanowski, E. Feldman, E. Wilson, G. Solbrekken, C. Jesse, J. Kennedy, J. Rivers and G. Schnieders, "Evaluation of Thin Plate Hydrodynamic Stability through a Combined Numerical Modeling and Experimental Effort," ANL/RTR/TM-16/9, Argonne National Laboratory, Lemont, IL, USA, May 2017.
- [26] W. Marcum, B. Woods, A. Phillips, R. Ambrosek and J. Wiest, "The OSU Hydro-Mechanical Fuel Test Facility: Standard Fuel Element Testing," in *RERTR 2010 - 32nd International Meeting on Reduced Enrichment for Research and Test Reactors*, Lisbon, Portugal, October 10-14, 2010.
- [27] A. Weiss, "OSU HMFTE - Instrumentation Uncertainty Analysis Report, Revision 4," OSU-HMFTE-100000-TECH-001, Oregon State University, Corvallis, OR, USA, February 2018.
- [28] Oregon State University, "The Hydro-Mechanical Fuel Test Facility," Oregon State University, [Online]. Available: <http://research.engr.oregonstate.edu/marcum/hmftf>. [Accessed 01 08 2021].
- [29] American Society of Mechanical Engineers, "Quality Assurance Requirements for Nuclear Facility Applications," ASME NQA-1-2008 with 2009 Addenda, American Society of Mechanical Engineers.
- [30] W. Jones, C. Jensen, D. Crawford, W. Marcum, A. Weiss, T. Howard and G. Latimer, "USHPRR Fuel Development Flow Testing Overview," in *RERTR 2016 - 37th International Meeting on Reduced Enrichment for Research and Test Reactors*, Antwerp, Belgium, October 23-27, 2016.

- [31] C. Jesse, W. Jones and A. Phillips, "Final Report on the Generic Test Plate Assembly Flow Test Campaign," INL/EXT-20-57793, Idaho National Laboratory, Idaho Falls, ID, USA, March 2020.
- [32] A. Weiss, "Generic Test Plate Assembly - Test Data Analysis Report," OSU-HMFTF-991000-TECH-005, Oregon State University, Corvallis, OR, USA, March 2020.
- [33] Oregon State University, "Oregon State University - Endurance Flow Loop," OSU, 2021. [Online]. Available: <http://research.engr.oregonstate.edu/marcum/efl>. [Accessed 01 08 2021].
- [34] R. Kmak, D. Jaluvka and E. Wilson, *LEU Fuel Element, Massachusetts Institute of Technology Reactor (MITR), R4F-100-000-4*, Cambridge, MA, USA: Massachusetts Institute of Technology Reactor, August 1, 2018.
- [35] R. Kmak, D. Jaluvka and E. Wilson, *Type F Fuel Plate, Massachusetts Institute of Technology Reactor (MITR), R4F-100-003-2*, Cambridge, MA, USA: Massachusetts Institute of Technology Reactor, August 1, 2018.
- [36] R. Kmak, D. Jaluvka and E. Wilson, *Side Plate, Massachusetts Institute of Technology Reactor (MITR), R4F-100-001-3*, Cambridge, MA, USA: Massachusetts Institute of Technology Reactor, August 1, 2018.
- [37] R. Kmak, D. Jaluvka and E. Wilson, *Nozzle End Fitting - Lower, Massachusetts Institute of Technology Reactor (MITR), R4F-100-004-3*, Cambridge, MA, USA: Massachusetts Institute of Technology Reactor, August 1, 2018.
- [38] G. Wang, C. Bojanowski, A. Hebden, D. Jaluvka and E. Wilson, "Massachusetts Institute of Technology Reactor LEU Element Flow Test Conceptual Design – Hydraulic Reactor Design Parameters," ANL/RTR/TM-21/17, Argonne National Laboratory, Lemont, IL, USA, September 2021.
- [39] K. Sun, A. J. Dave, L. Hu, E. H. Wilson, S. Pham, D. Jaluvka and T. Heltemes, "Transitional cores and fuel cycle analyses in support of MIT reactor low enriched uranium fuel conversion," *Progress in Nuclear Energy*, vol. 119, p. 103171, 2020.
- [40] A. J. Dave, K. Sun, L. Hu, S. H. Pham, E. H. Wilson and D. Jaluvka, "Thermal-hydraulic analyses of MIT reactor LEU transition cycles," *Progress in Nuclear Energy*, vol. 118, pp. 103-117, 2020.
- [41] W. Jones, W. Marcum, A. Weiss, C. Jensen, G. Hawkes, P. Murray, D. Crawford, J. Herter, J. Kennedy, N. Woolstenhulme, J. Weist, D. Chapman, T. Howard, G. Latimer and A. Phillips, "Reducing Uncertainty in Hydrodynamic Modeling of ATR Experiments Via Flow Testing Validation and Optimization," *Nuclear Technology*, vol. 201, pp. 286-303, 2018.
- [42] A. Weiss, "Development of a Strain Gage Program for the Measurement of Strain on Prototypic, Plate-type, High Performance Research Reactor Fuels under Flow Testing," Oregon State University, Corvallis, OR, USA, December 2017.
- [43] A. Weiss, "OSU HMFTF Channel Gap Probe," OSU-HMFTF-931000-SPEC-001, Oregon State University, Corvallis, OR, USA, March 2013.
- [44] A. Weiss, *Test Section, OSU-HMFTF-219000-DWG-001*, Corvallis, OR, USA: Oregon State University, February 2016.
- [45] A. Weiss, *Test Section - Upper Spool, OSU-HMFTF-219003-DWG-001*, Corvallis, OR, USA: Oregon State University, September 2014.
- [46] W. Marcum, *Test Section - Instrumentation Housing, OSU-HMFTF-219002-DWG-001*, Corvallis, OR, USA: Oregon State University, September 2014.

## Acknowledgment

The Massachusetts Institute of Technology Nuclear Reactor Laboratory is gratefully acknowledged for contributions to reactor conversion, including in the formation of the works referenced. The authors would like to thank Dr. Son Pham of Argonne National Laboratory for his valuable comments.

This work was sponsored by the U.S. Department of Energy, Office of Material Management and Minimization in the U.S. National Nuclear Security Administration Office of Defense Nuclear Nonproliferation under Contract DE-AC02-06CH11357.



## **Nuclear Science & Engineering Division**

Argonne National Laboratory  
9700 South Cass Avenue, Bldg. 208  
Argonne, IL 60439

[www.anl.gov](http://www.anl.gov)



Argonne National Laboratory is a U.S. Department of Energy  
laboratory managed by UChicago Argonne, LLC